IARC MONOGRAPHS

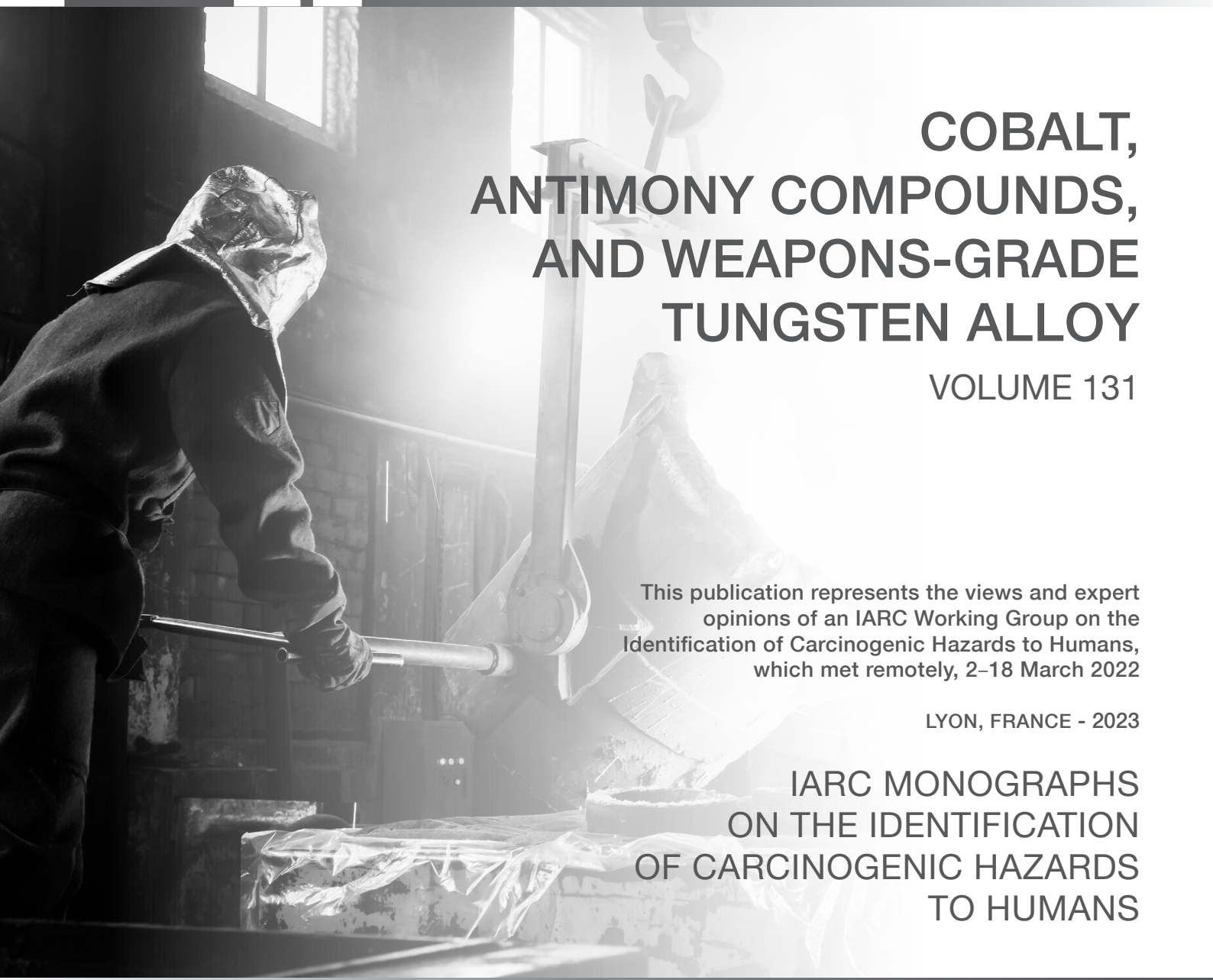

COBALT, ANTIMONY COMPOUNDS, AND WEAPONS-GRADE TUNGSTEN ALLOY

VOLUME 131

This publication represents the views and expert opinions of an IARC Working Group on the Identification of Carcinogenic Hazards to Humans, which met remotely, 2–18 March 2022

LYON, FRANCE - 2023

IARC MONOGRAPHS ON THE IDENTIFICATION OF CARCINOGENIC HAZARDS TO HUMANS

International Agency for Research on Cancer

World Health Organization

Table S4.14 Oxidative stress in non-human mammals in vivo exposed to cobalt

End-point	Species, strain, (sex)	Tissue	Results[a]	Direction of response	Dose (LED or HID)	Route, duration, dosing regimen	Comments	Reference
Cobalt metal								
Lipid peroxides, GSH, AOPP	Rat, SD (M)	Serum	–	No changes	1 cylinder of 1 mm in diameter by 2 mm in length/rat	Metal pellet implantation	Multiple time points tested following implantation.	Kalinich et al. (2022)
Cobalt(II) chloride ($CoCl_2$)								
MDA and/or HNE adduct formation	Rabbit, Albino (M)	Blood (erythrocyte and plasma)	+	↑	25 mg/kg [bw]/day	Subcutaneous, 3 days, 1×/day	A single dose tested with reasonable sample size.	Kuno et al. (1980)
	Rabbit, White (M)	Blood (erythrocyte and plasma)	+	↑	25 mg/kg [bw]/day	Subcutaneous, 3 days, 1×/day	A single dose tested with reasonable sample size.	Morita et al. (1982)
	Guinea-pig (M)	Liver	+	↑	80 mg/kg [bw]	Subcutaneous, 24 h, single dose	A single dose tested; Multiple end-points detected.	Christova et al. (2002)
	Rat, Wistar (M)	Liver	+	↑	10–60 mg/kg [bw]/day	Subcutaneous, 1–6 days, 1×/day	Multiple doses and durations tested.	Christova et al. (2001)
							A single dose tested; Multiple end-points detected.	Christova et al. (2002)
		Cardiac and renal tissues	+	↑	150, 300, 600 ppm	Oral administration (in drinking-water), 7 days	Dose-dependent effect.	Oyagbemi et al. (2019)
	Rat, Wistar (M + F)	Brain	+	↑	150 mg/kg [bw]/day	Oral gavage, 7 days, 1×/day, single dose	A single dose tested; Multiple end-points detected.	Akinrinde & Adebiyi (2019)
	Rat, Wistar (F)	Liver	+	↑	30 mg/kg [bw]	Intraperitoneal injection, 2 h, single dose	A single dose tested with reasonable sample size.	Sumbayev (2001)
					375 µmol/kg [bw]	Subcutaneous, 0–40 h, single dose	Time-dependent effect; $CoCl_2$ used as an oxidative stress inducer.	Gonzales et al. (2005)
	Rat, Wistar (F, pregnant and lactating)	F_0 and F_1 liver	+	↑	350 ppm	Oral administration (in drinking-water), started from day 14 of gestation until day 14 after delivery	A single dose tested; multiple end-points detected.	Garoui et al. (2011)
		Progeny cerebrum and cerebellum	+	↑	350 ppm	Oral administration (in drinking-water), started from day 14 of gestation until day 14 after delivery	A single dose tested; multiple end-points detected.	Garoui et al. (2013)

Table S4.14 (continued)

End-point	Species, strain, (sex)	Tissue	Results[a]	Direction of response	Dose (LED or HID)	Route, duration, dosing regimen	Comments	Reference
MDA and/or HNE adduct formation (cont.)	Rat, SD (M)	Brain	+	↑	50 mg/kg [bw]/day	Intragastric, 7 days, 1×/day	Cobalt prevents hypoxia-induced oxidative stress.	Shrivastava et al. (2008)
	Mouse, BDF_1 (M)	Liver	+	↑	60 mg/kg [bw]	Subcutaneous, 24 h, single dose	A single dose tested; multiple end-points detected.	Christova et al. (2003)
MDA	Rat, SD (M)	Red gastrocnemius muscle and plasma	+	↓	10 mg/kg [bw]/day (LED, 10 mg/kg [bw])	Oral administration, 15 days, 1×/day	$CoCl_2 \cdot 6H_2O$ used as hypoxia pre-treatment; a single dose tested with reasonable sample size; Multiple end-points detected.	Saxena et al. (2010)
Superoxide level	Rabbit, White (M)	Blood (erythrocyte and plasma)	+	↑	25 mg/kg [bw]/day	Subcutaneous, 3 days, 1×/day	A single dose tested with reasonable sample size.	Morita et al. (1982)
	Rabbit (M)	Alveolar macrophages in lung	+	↑	Cobalt: 0.4–2 µg/L	Inhalation, 14–16 wk (5 days/wk, 6 h/day)	Multiple doses test with reasonable sample size.	Johansson et al. (1986)
H_2O_2 level	Rat, Wistar (M)	Cardiac and renal tissues	+	↑	150–600 ppm	Oral administration (in drinking-water), 7 days	Dose-dependent effect.	Oyagbemi et al. (2019)
	Rat, Wistar (F)	Liver	(+)	↑	370 µmol/kg [bw]	Subcutaneous, 0–48 h, single dose	Time-dependent effect but no statistical difference.	Llesuy & Tomaro (1994)
	Rat, Wistar (M + F)	Brain	+	↑	150 mg/kg [bw]/day	Oral gavage, 7 days, 1×/day, single dose	A single dose tested; multi end-points detected.	Akinrinde & Adebiyi (2019)
	Rat, Wistar (F, pregnant and lactating)	Progeny cerebrum and cerebellum	+	↑	350 ppm	Oral administration (in drinking-water), started from day 14 of gestation until day 14 after delivery	A single dose tested; multiple end-points detected.	Garoui et al. (2013)
	Rat, SD (M)	Liver microsome	(+)	↓	30 mg /kg [bw]/day	Subcutaneous, 3 days, 1×/day	A single dose tested; limited samples (n = 2–6).	Daido & Aniya (1994)

Table S4.14 (continued)

End-point	Species, strain, (sex)	Tissue	Results[a]	Direction of response	Dose (LED or HID)	Route, duration, dosing regimen	Comments	Reference
NO level	Rat, Wistar (M)	Liver	+	↑	150–600 mg/L	Oral administration (in drinking-water), 7 days	Dose-dependent effect.	Awoyemi et al. (2017)
	Rat, Wistar (M + F)	Brain	+	↑	150 mg/kg [bw]/day	Oral gavage, 7 days, 1×/day, single dose	A single dose tested; multiple end-points detected.	Akinrinde & Adebiyi (2019)
	Rat, Wistar (M)	Cortex, cerebellum, and hippocampus	(+)	↑	Cobalt: 12.5 mg/kg [bw]/day	Oral administration, 7 days, 1×/day	$CoCl_2$ used as hypoxia mimic preconditioning.	Kalpana et al. (2008)
		Cardiac and renal tissues	+	↑	650 ppm	Oral administration (in drinking-water), 14 days	A single dose tested; Combination with antioxidant drugs.	Ajibade et al. (2017)
AOPP level	Wistar rats (M)	Liver	+	↑	150–600 mg/L	Oral administration (in drinking-water), 7 days	Dose-dependent effect.	Awoyemi et al. (2017)
		Cardiac and renal tissues	+	↑	150–600 ppm	Oral administration (in drinking-water), 7 days	Dose-dependent effect.	Oyagbemi et al. (2019)
	Rat, Wistar (F, pregnant and lactating)	Progeny cerebrum and cerebellum	+	↑	350 ppm	Oral administration (in drinking-water), started from the 14th days of pregnancy until day 14 after delivery	A single dose tested; multiple end-points detected.	Garoui et al. (2013)
ROS level	Rat, SD (M)	Brain	+	↓	50 mg/kg [bw]/day	Intragastric, 7 days, 1×/day	Cobalt prevents hypoxia-induced oxidative stress.	Shrivastava et al. (2008)
	Rat, Wistar (M)	Cortex, cerebellum, and hippocampus	(+)	↓	12.5 mg [bw]/day	Oral administration, 7 days, 1×/day	$CoCl_2$ used as hypoxia mimic preconditioning.	Kalpana et al. (2008)
PC level	Rat, Wistar (F, pregnant and lactating)	Progeny cerebrum and cerebellum	+	↑	350 ppm	Oral administration (in drinking-water), started from day 14 of gestation until day 14 after delivery	A single dose tested; multiple end-points detected including reduced V_c level.	Garoui et al. (2013)
	Rat, SD (M)	Brain	+	↓	50 mg/kg [bw]/day	Intragastric, 7 days, 1×/day	Cobalt prevents hypoxia-induced oxidative stress.	Shrivastava et al. (2008)

Table S4.14 (continued)

End-point	Species, strain, (sex)	Tissue	Results[a]	Direction of response	Dose (LED or HID)	Route, duration, dosing regimen	Comments	Reference
HO activity	Guinea-pig (M)	Liver	+	↑	80 mg/kg [bw]	Subcutaneous, 24 h, single dose	A single dose tested; multiple end-points detected.	Christova et al. (2002)
	Rat, Wistar (M)	Liver	+	↑	Cobalt: 125–375 µmol/kg [bw]	Subcutaneous, 1–24 h, single or multiple doses	Dose- and time interval-dependent effects; different repeated dosages effect; multiple administrations effect.	Numazawa et al. (1989a)
					10–60 mg/kg [bw]/day	Subcutaneous, 1–6 days, 1×/day	Multiple doses and durations were tested.	Christova et al. (2001)
					60 mg/kg [bw]	Subcutaneous, 24 h, single dose	A single dose tested; multiple end-points detected.	Christova et al. (2002)
	Rat, Wistar (F)	Liver	(+)	↑	370 µmol/kg [bw]	Subcutaneous, 0–48 h, single dose	Time-dependent effect but no statistical difference.	Llesuy & Tomaro (1994)
			+	↑	375 µmol/kg [bw]	Subcutaneous, 0–40 h, single dose	A single dose tested; $CoCl_2$ used as an oxidative stress inducer.	Gonzales et al. (2005)
	Rat, SD (M)	Liver	+	↑	60 mg/kg [bw]/day	Subcutaneous, 2 days, 1×/day	A single dose tested; limited sample size (n = 3).	Maines & Kappas (1974)
					250 µmol//kg [bw]	Subcutaneous, 4–48 h, single dose	$CoCl_2$ used as a potent inducer of HO; different duration was tested.	Kappas et al. (1985)
	Mouse, BDF_1 (M)	Liver	+	↑	60 mg/kg [bw]	Subcutaneous, 24 h, single dose	A single dose tested; multiple end-points detected.	Christova et al. (2003)
GPX activity	Guinea-pig (M)	Liver	+	↓	80 mg/kg [bw]	Subcutaneous, 24 h, single dose	A single dose tested; multiple end-points detected.	Christova et al. (2002)
	Mouse, BDF_1 (M)	Liver	+	↓	60 mg/kg [bw]	Subcutaneous, 24 h, single dose	A single dose tested; multiple end-points detected.	Christova et al. (2003)
	Rat, Wistar (M)	Myocardium	+	↓	1–50 mg/kg [bw]/day	Subcutaneous, 8 days, 1×/day	Dose-dependent effect.	Hatori et al. (1993)

Table S4.14 (continued)

End-point	Species, strain, (sex)	Tissue	Results[a]	Direction of response	Dose (LED or HID)	Route, duration, dosing regimen	Comments	Reference
GPX activity (cont.)	Rat, Wistar (M)	Liver	+	↓	10–60 mg/kg [bw]/day	Subcutaneous, 1–6 days, 1×/day	Multiple doses and durations tested.	Christova et al. (2001)
					150–600 mg/L	Oral administration (in drinking-water), 7 days	Dose-dependent effect.	Awoyemi et al. (2017)
		Cardiac and renal tissues	+	↓	650 ppm	Oral administration (in drinking-water), 14 days	A single dose tested; combination with antioxidant drugs.	Ajibade et al. (2017)
					150–600 ppm	Oral administration (in drinking-water), 7 days	Dose-dependent effect.	Oyagbemi et al. (2019)
	Rat, Wistar (M + F)	Brain	+	↓	150 mg/kg [bw]/day	Oral gavage, 7 days, 1×/day, single dose	A single dose tested; Multiple end-points detected.	Akinrinde & Adebiyi (2019)
	Rat, Wistar (F)	Liver	(+)	↓	370 µmol/kg [bw]	Subcutaneous, 0–48 h, single dose	Time-dependent effect but no statistical difference.	Llesuy & Tomaro (1994)
			+	↓	375 µmol/kg [bw]	Subcutaneous, 12 h, single dose	A single dose tested; $CoCl_2$ used as an oxidative stress inducer.	Gonzales et al. (2005)
	Rat, Wistar (F, pregnant and lactating)	F_0 and F_1 liver	+	↓	350 ppm	Oral administration (in drinking-water), started from day 14 of gestation until day 14 after delivery	A single dose tested; multiple end-points detected.	Garoui et al. (2011)
	Rat, Wistar (F, pregnant and lactating)	Progeny cerebrum and cerebellum	+	↓	350 ppm	Oral administration (in drinking-water), started from day 14 of gestation until day 14 after delivery	A single dose tested; multiple end-points detected.	Garoui et al. (2013)
	Rat, SD (M)	Liver microsome	+	↓	30 mg/kg [bw]/day	Subcutaneous, 0–24 h, single dose	Time-dependent effects.	Daido & Aniya (1994)
					30–60 mg/kg [bw]/day	Subcutaneous, 3 days, 1×/day	Dose-dependent effects.	Daido & Aniya (1994)
		Brain	+	↓	50 mg/kg [bw]/day	Intragastric, 7 days, 1×/day	Cobalt prevents hypoxia-induced oxidative stress.	Shrivastava et al. (2008)

Table S4.14 (continued)

End-point	Species, strain, (sex)	Tissue	Results[a]	Direction of response	Dose (LED or HID)	Route, duration, dosing regimen	Comments	Reference
GPX activity (cont.)		Red gastrocnemius muscle	+	↓	10 mg/kg [bw]/day (LED, 10 mg/kg [bw])	Oral administration, 15 days	$CoCl_2 \cdot 6H_2O$ used as hypoxia pre-treatment; a single dose tested with reasonable sample size; Multiple end-points detected.	Saxena et al. (2010)
GST activity	Rat, SD (M)	Liver microsome	+	↑	30–60 mg/kg [bw]/day	Subcutaneous, 3 days, 1×/day	Dose-dependent effect.	Daido & Aniya (1994)
					60 mg/kg [bw]	Subcutaneous, 0–24 h, single dose	Time-dependent effect.	Daido & Aniya (1994)
	Rat, Wistar (M)	Liver	+	↓	150–600 mg/L	Oral administration (in drinking-water), 7 days	Dose-dependent effect.	Awoyemi et al. (2017)
		Cardiac and renal tissues	+	↓	150–600 ppm [150–600 mg/L]	Oral administration (in drinking-water), 7 days	Dose-dependent effect.	Oyagbemi et al. (2019)
	Rats, SD (M)	Brain	+	↓	50 mg/kg [bw]/day	Intragastric, 7 days, 1×/day	Cobalt prevents hypoxia-induced oxidative stress.	Shrivastava et al. (2008)
SOD activity	Guinea-pig (M)	Liver	+	↓	80 mg/kg [bw]	Subcutaneous, 24 h, single dose	A single dose tested; Multiple end-points detected.	Christova et al. (2002)
	Rat, Wistar (M)	Liver	+	↓	10–60 mg/kg [bw]/day	Subcutaneous, 1–6 days, 1×/day	Multiple doses and durations were tested.	Christova et al. (2001)
					150–600 mg/L	Oral administration (in drinking-water), 7 days	Dose-dependent effect.	Awoyemi et al. (2017)
		Brain	+	↓	40 mg/kg [bw]/day	Oral gavage, 60 days, 1×/day, single dose	$CoCl_2$ used as hypoxia mimic; a single dose tested; multiple end-points detected.	Abdel-Rahman Mohamed et al. (2019)
	Rat, Wistar (F)	Liver	(+)	↓	370 µmol/kg [bw]	Subcutaneous, 0–48 h, single dose	Time-dependent effect but no statistical difference.	Llesuy & Tomaro (1994)
			+	↓	375 µmol/kg [bw]	Subcutaneous, 12 h, single dose	A single dose tested; $CoCl_2$ used as an oxidative stress inducer.	Gonzales et al. (2005)

Table S4.14 (continued)

End-point	Species, strain, (sex)	Tissue	Results[a]	Direction of response	Dose (LED or HID)	Route, duration, dosing regimen	Comments	Reference
SOD activity (cont.)	Rat, Wistar (F, pregnant and lactating)	F_0 and F_1 liver	+	↓	350 ppm	Oral administration (in drinking-water), started from day 14 of gestation until day 14 after delivery	A single dose tested; Multiple end-points detected.	Garoui et al. (2011)
		Progeny cerebrum and cerebellum	+	↓	350 ppm	Oral administration (in drinking-water), started from day 14 of gestation until day 14 after delivery	A single dose tested; multiple end-points detected.	Garoui et al. (2013)
	Rat, Wistar (M + F)	Brain	+	↓	150 mg/kg [bw]/day	Oral gavage, 7 days, 1×/day, single dose	A single dose tested; multiple end-points detected.	Akinrinde & Adebiyi (2019)
	Rat, SD (M)	Brain	+	↓	50 mg/kg [bw]/day	Intragastric, 7 days, 1×/day	Cobalt prevents hypoxia-induced oxidative stress.	Shrivastava et al. (2008)
	Mouse, BDF_1 (M)	Liver	+	↓	60 mg/kg [bw]	Subcutaneous, 24 h, single dose	A single dose tested; multiple end-points detected.	Christova et al. (2003)
Mn-SOD activity	Rat, Wistar (M)	Myocardium	+	↓	1–50 mg/kg [bw]/day	Subcutaneous, 8 days, 1×/day	Dose-dependent effect.	Hatori et al. (1993)
CAT activity	Guinea-pig (M)	Liver	+	↑	80 mg/kg [bw]	Subcutaneous, 24 h, single dose	A single dose tested; multiple end-points detected.	Christova et al. (2002)
	Rat, Wistar (M)	Liver	+	↓	10–60 mg/kg [bw]/day	Subcutaneous, 1–6 days, 1×/day	Multiple doses and durations tested.	Christova et al. (2001)
					150–600 mg/L	Oral administration (in drinking-water), 7 days	Dose-dependent effect.	Awoyemi et al. (2017)
		Brain	+	↓	40 mg/kg [bw]/day	Oral gavage, 60 days, 1×/day, single dose	$CoCl_2$ used as hypoxia mimic; a single dose tested; multiple end-points detected.	Abdel-Rahman Mohamed et al. (2019)
		Cardiac and renal tissues	+	↓	150–600 ppm	Oral administration (in drinking-water), 7 days	Dose-dependent effect.	Oyagbemi et al. (2019)
	Rat, Wistar (F)	Liver	(+)	↓	370 µmol/kg [bw]	Subcutaneous, 0–48 h, single dose	Time-dependent effect but no statistical difference.	Llesuy & Tomaro (1994)
			+	↓	375 µmol/kg [bw]	Subcutaneous, 12 h, single dose	A single dose tested; $CoCl_2$ used as an oxidative stress inducer.	Gonzales et al. (2005)

Table S4.14 (continued)

End-point	Species, strain, (sex)	Tissue	Results[a]	Direction of response	Dose (LED or HID)	Route, duration, dosing regimen	Comments	Reference
CAT activity (cont.)	Rat, Wistar (F, pregnant and lactating)	F_0 and F_1 liver	+	↓	350 ppm	Oral administration (in drinking-water), started from day 14 of gestation until day 14 after delivery	A single dose tested; Multiple end-points detected.	Garoui et al. (2011)
		Progeny cerebrum and cerebellum	+	↓	350 ppm	Oral administration (in drinking-water), started from day 14 of gestation until day 14 after delivery	A single dose tested; multiple end-points detected.	Garoui et al. (2013)
	Mouse, BDF_1 (M)	Liver	+	↓	60 mg/kg [bw]	Subcutaneous, 24 h, single dose	A single dose tested; multiple end-points detected.	Christova et al. (2003)
GR activity	Guinea-pig (M)	Liver	+	↑	80 mg/kg [bw]	Subcutaneous, 24 h, single dose	A single dose tested; multiple end-points detected.	Christova et al. (2002)
	Rat, Wistar (M)	Liver	+	↑	10–60 mg/kg [bw]/day	Subcutaneous, 1–6 days, 1×/day	Multiple doses and durations were tested.	Christova et al. (2001)
					60 mg/kg [bw]	Subcutaneous, 24 h, single dose	A single dose tested; multiple end-points detected.	Christova et al. (2002)
GSH level	Rat, Wistar (M)	Liver	+	↑	10–30 mg/kg [bw]/day	Subcutaneous, 2–6 days, 1×/day	Multiple doses and durations tested	Christova et al. (2001)
	Rat, SD (M)	Liver	+	↑	45 mg/kg [bw]	Subcutaneous, single dose after fasted for 48 h	$CoCl_2$ used to regulate GSH content; set the contrast.	Nordström et al. (1990)
		Red gastrocnemius muscle	+	↑	10 mg/kg [bw]/day (LED, 10 mg/kg [bw])	Oral administration, 15 days, 1×/day	$CoCl_2 \cdot 6H_2O$ used as hypoxia pre-treatment; a single dose tested with reasonable sample size; multiple end-points detected.	Saxena et al. (2010)
	Guinea-pig (M)	Liver	+	↓	80 mg/kg [bw]	Subcutaneous, 24 h, single dose	A single dose tested; multiple end-points detected.	Christova et al. (2002)
	Rat, Wistar (M)	Liver	+	↓	60 mg/kg [bw]/day	Subcutaneous, 1 day, 1×/day	Multiple doses and duration tested.	Christova et al. (2001)
		Cardiac and renal tissues	+	↓	650 ppm	Oral administration (in drinking-water), 14 days	A single dose tested; combination with antioxidant drugs.	Ajibade et al. (2017)
					150–600 ppm	Oral administration (in drinking-water), 7 days	Dose-dependent effect.	Oyagbemi et al. (2019)

Table S4.14 (continued)

End-point	Species, strain, (sex)	Tissue	Results[a]	Direction of response	Dose (LED or HID)	Route, duration, dosing regimen	Comments	Reference
GSH level (cont.)		Brain	+	↓	40 mg/kg [bw]/day	Oral gavage, 60 days, 1×/day, single dose	$CoCl_2$ used as hypoxia mimic; a single dose tested; multiple end-points detected.	Abdel-Rahman Mohamed et al. (2019)
	Rat, Wistar (F)	Liver	+	↓	375 µmol/kg [bw]	Subcutaneous, 0–40 h, single dose	Time-dependent effect; $CoCl_2$ used as an oxidative stress inducer.	Gonzales et al. (2005)
	Rat, Wistar (F, pregnant and lactating)	F0 and F1 liver	+	↓	350 ppm	Oral administration (in drinking-water), started from day 14 of gestation until day 14 after delivery	A single dose tested; multiple end-points detected.	Garoui et al. (2011)
		Progeny cerebrum and cerebellum	+	↓	350 ppm	Oral administration (in drinking-water), started from day 14 of gestation until day 14 after delivery	A single dose tested; multiple end-points detected.	Garoui et al. (2013)
	Rat, Wistar (M + F)	Brain	+	↓	150 mg/kg [bw]/day	Oral gavage, 7 days, 1×/day, single dose	A single dose tested; multiple end-points detected.	Akinrinde & Adebiyi (2019)
	Rat, SD (M)	Brain	+	↓	50 mg/kg [bw]/day	Intragastric, 7 days, 1×/day	Cobalt prevents hypoxia-induced oxidative stress.	Shrivastava et al. (2008)
	Mouse, BDF_1 (M)	Liver	+	↓	60 mg/kg [bw]	Subcutaneous, 24 h, single dose	A single dose tested; multiple end-points detected.	Christova et al. (2003)
	Rat, Wistar (F)	Liver	(+)	↓	370 µmol/kg [bw]	Subcutaneous, 0–48 h, single dose	Time-dependent effect but no statistical difference.	Llesuy & Tomaro (1994)
GSSG level	Rat, SD (M)	Brain	+	↓	50 mg/kg [bw]/day	Intragastric, 7 days, 1×/day	Cobalt prevents hypoxia-induced oxidative stress.	Shrivastava et al. (2008)
GSH/ GSSG ratio	Rat, SD (M)	Brain	+	↑	50 mg/kg [bw]/day	Intragastric, 7 days, 1×/day	Cobalt prevents hypoxia-induced oxidative stress.	Shrivastava et al. (2008)
		Red gastrocnemius muscle	+	↑	10 mg/kg [bw]/day (LED, 10 mg/kg [bw])	Oral administration, 15 days	$CoCl_2 \cdot 6H_2O$ used as hypoxia pre-treatment; a single dose tested with reasonable sample size; multiple end-points detected.	Saxena et al. (2010)
PSH level	Rat, Wistar (M)	Renal tissues	+	↑	150–600 ppm	Oral administration (in drinking-water), 7 days	Dose-dependent effect and peaks at 600 ppm.	Oyagbemi et al. (2019)

Table S4.14 (continued)

End-point	Species, strain, (sex)	Tissue	Results[a]	Direction of response	Dose (LED or HID)	Route, duration, dosing regimen	Comments	Reference
PSH level (cont.)	Rat, Wistar (M)	Cardiac and renal tissues	+	↓	650 ppm	Oral administration (in drinking-water), 14 days	A single dose tested; combination with antioxidant drugs.	Ajibade et al. (2017)
NPSH level	Rat, Wistar (M)	Cardiac and renal tissues	+	↓	650 ppm	Oral administration (in drinking-water), 14 days	A single dose tested; combination with antioxidant drugs.	Ajibade et al. (2017)
	Rat, Wistar (F, pregnant and lactating)	Progeny cerebrum and cerebellum	+	↓	350 ppm	Oral administration (in drinking-water), started from day 14 of gestation until day 14 after delivery	A single dose tested; multiple end-points detected.	Garoui et al. (2013)
HO-1 level	Rat, Wistar (F)	Liver	+	↑	375 µmol/kg [bw]	Subcutaneous, 0–40 h, single dose	A single dose tested; $CoCl_2$ used as an oxidative stress induce.	Gonzales et al. (2005)
	SD rats (M)	Liver	+	↑	300 µmol/kg [bw]	Subcutaneous, 6 h, single dose	A single dose tested.	Bauer et al. (1998)
		Red gastrocnemius muscle	+	↑	10 mg/kg [bw]/day (LED, 10 mg/kg [bw])	Oral administration, 15 days, 1×/day	$CoCl_2 \cdot 6H_2O$ used as hypoxia pre-treatment; a single dose tested with reasonable sample size; multiple end-points detected.	Saxena et al. (2010)
		Kidney	+	↑	20 mg/kg [bw]/day	Oral gavage, 4 wk, 1×/day, single dose	$CoCl_2$ used as hypoxia mimic; a single dose tested.	Nordquist et al. (2015)
HO-2 level	SD rats (M)	Liver	+	↑	300 µmol/kg [bw]	Subcutaneous, 6 h, single dose	A single dose tested.	Bauer et al. (1998)
Cu/Zn-SOD level	SD rats (M)	Kidney	+	↑	20 mg/kg [bw]/day	Oral gavage, 4 wk, 1×/day, single dose	$CoCl_2$ used as hypoxia mimic; a single dose tested.	Nordquist et al. (2015)
NOX2 level	Rat, Wistar (M)	Brain	+	↑	50 mmol/day	Surgically injected into brain, 1–5 days	$CoCl_2$ used as hypoxia mimic.	Guan et al. (2015)
Nrf2 level	Rat, Wistar (M)	Brain	+	↓	50 mmol/day	Surgically injected into brain, 1–5 days	$CoCl_2$ used as hypoxia mimic.	Guan et al. (2015)

Table S4.14 (continued)

End-point	Species, strain, (sex)	Tissue	Results[a]	Direction of response	Dose (LED or HID)	Route, duration, dosing regimen	Comments	Reference
Cobalt(II) chloride hexahydrate ($CoCl_2 \cdot 6H_2O$)								
MDA	Rat, Wistar (M)	Kidneys, heart	+	↑	350 ppm	Oral administration (in drinking-water), 7 days	A single dose tested; multiple end-points detected.	Akinrinde et al. (2016)
		Hippocampus	+	↑	4 mg/kg [bw]/day	Intraperitoneal injection, 20 days, 1×/day	A single dose tested; multiple end-points detected.	Zheng et al. (2019)
		Liver	+	↑	150–600 mg/L	Oral administration (in drinking-water), 7 days	Dose-dependent effect.	Awoyemi et al. (2017)
		Cardiac and renal tissues	+	↑	150 mg/kg [bw]/day	Intragastric, 8 days, 1×/day	A single dose tested; multiple end-points detected.	Oyagbemi et al. (2020)
	Rat, SD (M)	Kidney	+	↑	300 mg/L	Oral administration (in drinking-water), 28 days	A single dose tested; multiple end-points detected.	Abdel-Daim et al. (2020)
H_2O_2 level	Rat, Wistar (M)	Kidneys, heart	+	↑	350 ppm	Oral administration (in drinking-water), 7 days	A single dose tested; multiple end-points detected.	Akinrinde et al. (2016)
		Liver	+	↑	150–600 mg/L	Oral administration (in drinking-water), 7 days	Dose-dependent effect.	Awoyemi et al. (2017)
		Cardiac and renal tissues	+	↑	150 mg/kg [bw]/day	Intragastric, 8 days, 1×/day	A single dose tested; multiple end-points detected.	Oyagbemi et al. (2020)
	Rat, SD (M)	Kidney	+	↑	300 mg/L	Oral administration (in drinking-water), 28 days	A single dose tested; multiple end-points detected.	Abdel-Daim et al. (2020)
NO level	Rat, Wistar (M)	Cardiac tissues	+	↑	150 mg/kg [bw]/day	Intragastric, 8 days, 1×/day	A single dose tested; multiple end-points detected.	Oyagbemi et al. (2020)
	Rat, SD (M)	Kidney	+	↑	300 mg/L	Oral administration (in drinking-water), 28 days	A single dose tested; multiple end-points detected.	Abdel-Daim et al. (2020)
ROS level	Rat, SD (M)	Liver	+	↑	300 mg/L	Oral administration (in drinking-water), 28 days	A single dose tested; multiple end-points detected.	Khalil et al. (2020)
8-OHdG level	Rat, SD (M)	Kidney	+	↑	300 mg/L	Oral administration (in drinking-water), 28 days	A single dose tested; multiple end-points detected.	Abdel-Daim et al. (2020)
Free radical level	Rat, SD (M)	Blood	+	↑	50 mM	Intravenous injection, 40 min continuously (at a rate of 23.3 µL/min)	Time-dependent effects.	Wang et al. (1993)
TAC	Rat, SD (M)	Liver	+	↓	300 mg/L	Oral administration (in drinking-water), 28 days	A single dose tested; multiple end-points detected.	Khalil et al. (2020)
PC level	Rat, SD (M)	Liver	+	↑	300 mg/L	Oral administration (in drinking-water), 28 days	A single dose tested; multiple end-points detected.	Khalil et al. (2020)

Table S4.14 (continued)

End-point	Species, strain, (sex)	Tissue	Results[a]	Direction of response	Dose (LED or HID)	Route, duration, dosing regimen	Comments	Reference
HO activity	Rat, SD (M)	Liver and bile	+	↑	250 µmol/kg [bw]	Subcutaneous, 1–72 h, single dose	Time-dependent effect.	Stelzer & Klaassen (1985)
	Rat, Wistar	Liver	+	↑	3 mg/100 g [bw]	Subcutaneous, 2–24 h, single dose	A single dose tested with reasonable sample size.	Kaliman et al. (2001)
GPX activity	Rat, Wistar (M)	Cardiac and renal tissues	+	↓	150 mg/kg [bw]/day	Intragastric, 8 days, 1×/day	A single dose tested; multiple end-points detected.	Oyagbemi et al. (2020)
GST activity	Rat, Wistar (M)	Heart	+	↑	350 ppm	Oral administration (in drinking-water), 7 days	A single dose tested; multiple end-points detected.	Akinrinde et al. (2016)
	Rat, Wistar (M)	Renal tissues	+	↓	150 mg/kg [bw]/day	Intragastric, 8 days, 1×/day	A single dose tested; multiple end-points detected.	Oyagbemi et al. (2020)
SOD activity	Rat, Wistar (M)	Kidney	+	↓	350 ppm	Oral administration (in drinking-water), 7 days	A single dose tested; multiple end-points detected.	Akinrinde et al. (2016)
	Rat, SD (M)	Kidney	+	↓	300 mg/L	Oral administration (in drinking-water), 28 days	A single dose tested; multiple end-points detected.	Abdel-Daim et al. (2020)
CAT activity	Rat, Wistar (M)	Heart	+	↑	350 ppm	Oral administration (in drinking-water), 7 days	A single dose tested; multiple end-points detected.	Akinrinde et al. (2016)
	Rat, SD (M)	Kidney	+ ↓	↓	300 mg/L	Oral administration (in drinking-water), 28 days	A single dose tested; multiple end-points detected.	Abdel-Daim et al. (2020)
MPO activity	Rat, Wistar (M)	Serum	+	↑	150 mg/kg [bw]/day	Intragastric, 8 days, 1×/day	A single dose tested; multiple end-points detected.	Oyagbemi et al. (2020)
GSH level	Rat, SD (M)	Bile	+	↑	250 µmol/kg [bw]	Subcutaneous, 1–72 h, single dose	Time-dependent effect.	Stelzer & Klaassen (1985)

Table S4.14 (continued)

End-point	Species, strain, (sex)	Tissue	Results[a]	Direction of response	Dose (LED or HID)	Route, duration, dosing regimen	Comments	Reference
GSH level (cont.)	Syrian golden hamster, (M or F)	Lung	+	↓	1–10 000 µg/kg [bw]	Intratracheal instillation, 3–48 h, single dose	Dose-dependent effect.	Lewis et al. (1991)
	Rat, Wistar (M)	Kidneys, heart	+	↑	350 ppm	Oral administration (in drinking-water), 7 days	A single dose tested; multiple end-points detected.	Akinrinde et al. (2016)
		Cardiac and renal tissues	+	↑	150 mg/kg [bw]/day	Intragastric, 8 days, 1×/day	A single dose tested; multiple end-points detected.	Oyagbemi et al. (2020)
	Rat, SD (M)	Kidney	+	↑	300 mg/L	Oral administration (in drinking-water), 28 days	A single dose tested; multiple end-points detected.	Abdel-Daim et al. (2020)
GSSG level	Syrian golden Hamsters (M or F)	Lung	+	↑	1–10 000 µg/kg [bw]	Intratracheal instillation, 3–48 h, single dose	Dose-dependent effect.	Lewis et al. (1991)
	Rat, SD (M)	Bile	+	↑	250 µmol/kg [bw]	Subcutaneous, 1–72 h, single dose	Time-dependent effect.	Stelzer & Klaassen (1985)
Nrf2 level	Rat, Wistar (M)	Hippocampus	+	↑	4 mg/kg [bw]/day	Intraperitoneal injection, 20 days, 1×/day	A single dose tested; multiple end-points detected.	Zheng et al. (2019)
HO-1 level	Rat, Wistar (M)	Substantia nigra Hippocampus	+	↑	4 mg/kg [bw]/day	Intraperitoneal injection, 20 days, 1×/day	A single dose tested; multiple end-points detected.	Zheng et al. (2019)
MPO level	Rat, SD (M)	Kidney	+	↑	300 mg/L	Oral administration (in drinking-water), 28 days	A single dose tested; multiple end-points detected.	Abdel-Daim et al. (2020)
Cobalt(II) sulfate heptahydrate ($CoSO_4 \cdot 7H_2O$)								
Mn-SOD activity	Rat, SD (M)	Myocardium	+ ↓	↓	40 mg/kg [bw]	Oral administration (in feed), 24 wk	A single dose tested with reasonable sample size.	Clyne et al. (2001)
Cobalt(II) acetate ($C_4H_6CoO_4$)								
Oxidative DNA damage	Rat, F344/NCr (M + F)	Kidney, liver, and lung	+	↑	50–100 µM/kg [bw]	Intraperitoneal injection, 2–10 days, single dose	Dose-dependent effect.	Kasprzak et al. (1994)

Table S4.14 (continued)

End-point	Species, strain, (sex)	Tissue	Results[a]	Direction of response	Dose (LED or HID)	Route, duration, dosing regimen	Comments	Reference
Ultrafine cobalt metal								
Lipid peroxides	Rat, Wistar (M)	BALF	+	↑	1 mg ultrafine cobalt metallic particles with a mean diameter of 20 nm/rat	Intratracheal instillation		Zhang et al. (1998)
Ultrafine cobalt(II,III) oxide (Co_3O_4)								
Hydroxyl radical generation	Rat, Wistar (M)	BALF	(+)	↑	Co_3O_4: 125 µg/rat	Intratracheal instillation, 4–18 h, single dose	A single dose tested; limited samples (n = 3).	Dick et al. (2003)
Cobalt-based NPs								
MDA level	Rat, Wistar (M)	Temporal lobe and hippocampus	+	↑	Cobalt metal NPs (size, 96 nm): 2–8 mg/kg [bw]/day	Intraperitoneal injection, 20 days, 1×/day	Dose-dependent effect.	Zheng et al. (2019)
8-OHdG level	Mouse, Gpt delta transgenic mice	Lung	+	↑	85–90% cobalt metal and 10–15% Co_3O_4 NPs: 50 µg/mouse	Intratracheal instillation, 1–28 days, single dose	A single dose tested; different durations tested.	Wan et al. (2017)
NRF2 level	Rat, Wistar (M)	Hippocampus	+	↑	Cobalt metal NPs (size, 96 nm): 2–8 mg/kg [bw]/day	Intraperitoneal injection, 20 days, 1×/day	Dose-dependent effect.	Zheng et al. (2019)
HO-1 level	Mouse, C57BL/6 (M)	Lung	+	↑	CoO NPs (size < 100 nm): 20 µg/mouse	Oropharyngeal aspiration, 40 h, single dose	A single dose tested; combine multiple analysis methods.	Zhang et al. (2012)
	Rat, Wistar (M)	Hippocampus	+	↑	Cobalt metal NPs (size, 96 nm): 2–8 mg/kg [bw]/day	Intraperitoneal injection, 20 days, 1×/day	Dose-dependent effect.	Zheng et al. (2019)

Table S4.14 (continued)

End-point	Species, strain, (sex)	Tissue	Results[a]	Direction of response	Dose (LED or HID)	Route, duration, dosing regimen	Comments	Reference
8-oxo-dG level	Mouse, B6C3F1/N (M) and (F)	Lung	+	↑	Cobalt metal dust (high dose, 10 mg/m^3)	Inhalation, 90 days		Ton et al. (2021)

4-HNE, 4-hydroxynonenal; 8-OHdG, 8-hydroxy-2′-deoxyguanosine; AOPP, advanced oxidation protein products; BALF, bronchoalveolar lavage fluid; bw, body weight; CAT, catalase; Cu/Zn-SOD, copper/zinc superoxide dismutase; F, female; Gpt, guanine phosphoribosyltransferase; GPX, glutathione peroxidase; GR, glutathione reductase; GSH, glutathione; GSSG, oxidized glutathione; GST, glutathione *S*-transferase; HID, highest ineffective dose; HO, haem oxygenase; HO-1, haem oxygenase isoenzyme 1; HO-2, haem oxygenase isoenzyme 2; H_2O_2, hydrogen peroxide; LED, lowest effective dose; M, male; MDA, malondialdehyde; min, minute; Mn-SOD, manganese superoxide dismutase; MPO, myeloperoxidase; NO, nitric oxide; NOX2, NADPH oxidase 2; NPSH, non-protein thiol; Nrf2, nuclear factor E2-related factor 2; PC, protein carbonyl; ppm, parts per million; PSH, protein thiol; ROS, reactive oxygen species; SD, Sprague-Dawley; SOD, superoxide dismutase; TAC, total antioxidant capacity; V_C, vitamin C; wk, week.

[a] +, positive; –, negative; (+) or (–), positive or negative in a study of limited quality; ↓, decrease; ↑, increase.

References

Abdel-Daim MM, Khalil SR, Awad A, Abu Zeid EH, El-Aziz RA, El-Serehy HA (2020). Ethanolic extract of *Moringa oleifera* leaves influences NF-κB signaling pathway to restore kidney tissue from cobalt-mediated oxidative injury and inflammation in rats. *Nutrients*. 12(4):1031. doi:10.3390/nu12041031 PMID:32283757

Abdel-Rahman Mohamed A, Metwally MMM, Khalil SR, Salem GA, Ali HA (2019). *Moringa oleifera* extract attenuates the $CoCl_2$ induced hypoxia of rat's brain: expression pattern of HIF-1α, NF-kB, MAO and EPO. *Biomed Pharmacother*. 109:1688–97. doi:10.1016/j.biopha.2018.11.019 PMID:30551423

Ajibade TO, Oyagbemi AA, Omobowale TO, Asenuga ER, Adigun KO (2017). Quercetin and vitamin C mitigate cobalt chloride-induced hypertension through reduction in oxidative stress and nuclear factor kappa beta (NF-Kb) expression in experimental rat model. *Biol Trace Elem Res*. 175(2):347–59. doi:10.1007/s12011-016-0773-5 PMID:27283837

Akinrinde AS, Adebiyi OE (2019). Neuroprotection by luteolin and gallic acid against cobalt chloride-induced behavioural, morphological and neurochemical alterations in Wistar rats. *Neurotoxicology*. 74:252–63. doi:10.1016/j.neuro.2019.07.005 PMID:31362009

Akinrinde AS, Oyagbemi AA, Omobowale TO, Asenuga ER, Ajibade TO (2016). Alterations in blood pressure, antioxidant status and caspase 8 expression in cobalt chloride-induced cardio-renal dysfunction are reversed by *Ocimum gratissimum* and gallic acid in Wistar rats. *J Trace Elem Med Biol*. 36:27–37. doi:10.1016/j.jtemb.2016.03.015 PMID:27259349

Alinovi R, Goldoni M, Pinelli S, Campanini M, Aliatis I, Bersani D, et al. (2015). Oxidative and pro-inflammatory effects of cobalt and titanium oxide nanoparticles on aortic and venous endothelial cells. *Toxicol In Vitro*. 29(3):426–37. doi:10.1016/j.tiv.2014.12.007 PMID:25526690

Alzhrani RM, Alhadidi Q, Bachu RD, Shah Z, Dey S, Boddu SHS (2017). Tanshinone IIA inhibits VEGF secretion and HIF-1α expression in cultured human retinal pigment epithelial cells under hypoxia. *Curr Eye Res*. 42(12):1667–73. doi:10.1080/02713683.2017.1355467 PMID:28937825

Anard D, Kirsch-Volders M, Elhajouji A, Belpaeme K, Lison D (1997). In vitro genotoxic effects of hard metal particles assessed by alkaline single cell gel and elution assays. *Carcinogenesis*. 18(1):177–84. doi:10.1093/carcin/18.1.177 PMID:9054604

Anjum SA, Lawrence H, Holland JP, Kirby JA, Deehan DJ, Tyson-Capper AJ (2016). Effect of cobalt-mediated toll-like receptor 4 activation on inflammatory responses in endothelial cells. *Oncotarget*. 7(47):76471–8. doi:10.18632/oncotarget.13260 PMID:27835611

Arlauskas A, Baker RSU, Bonin AM, Tandon RK, Crisp PT, Ellis J (1985). Mutagenicity of metal ions in bacteria. *Environ Res*. 36(2):379–88. doi:10.1016/0013-9351(85)90032-5 PMID:3884331

Awoyemi OV, Okotie UJ, Oyagbemi AA, Omobowale TO, Asenuga ER, Ola-Davies OE, et al. (2017). Cobalt chloride exposure dose-dependently induced hepatotoxicity through enhancement of cyclooxygenase-2 (COX-2)/B-cell associated protein X (BAX) signaling and genotoxicity in Wistar rats. *Environ Toxicol*. 32(7):1899–907. doi:10.1002/tox.22412 PMID:28303633

Bae S, Jeong HJ, Cha HJ, Kim K, Choi YM, An IS, et al. (2012). The hypoxia-mimetic agent cobalt chloride induces cell cycle arrest and alters gene expression in U266 multiple myeloma cells. *Int J Mol Med*. 30(5):1180–6. doi:10.3892/ijmm.2012.1115 PMID:22941251

Balaiya S, Murthy RK, Chalam KV (2013). Resveratrol inhibits proliferation of hypoxic choroidal vascular endothelial cells. *Mol Vis*. 19:2385–92. PMID:24319332

Barrak NH, Khajah MA, Luqmani YA (2020). Hypoxic environment may enhance migration/penetration of endocrine resistant MCF7- derived breast cancer cells through monolayers of other non-invasive cancer cells in vitro. *Sci Rep*. 10(1):1127. doi:10.1038/s41598-020-58055-x PMID:31980706

Bauer I, Wanner GA, Rensing H, Alte C, Miescher EA, Wolf B, et al. (1998). Expression pattern of heme oxygenase isoenzymes 1 and 2 in normal and stress-exposed rat liver. *Hepatology*. 27(3):829–38. doi:10.1002/hep.510270327 PMID:9500714

Bi S, Liu JR, Li Y, Wang Q, Liu HK, Yan YG, et al. (2010). γ-Tocotrienol modulates the paracrine secretion of VEGF induced by cobalt(II) chloride via ERK signaling pathway in gastric adenocarcinoma SGC-7901 cell line. *Toxicology*. 274(1–3):27–33. doi:10.1016/j.tox.2010.05.002 PMID:20452389

Busch W, Kühnel D, Schirmer K, Scholz S (2010). Tungsten carbide cobalt nanoparticles exert hypoxia-like effects on the gene expression level in human keratinocytes. *BMC Genomics*. 11(1):65. doi:10.1186/1471-2164-11-65 PMID:20105288

Caicedo MS, Pennekamp PH, McAllister K, Jacobs JJ, Hallab NJ (2010). Soluble ions more than particulate cobalt-alloy implant debris induce monocyte costimulatory molecule expression and release of proinflammatory cytokines critical to metal-induced lymphocyte reactivity. *J Biomed Mater Res A*. 93(4):1312–21. PMID:19844976

Cavallo D, Ciervo A, Fresegna AM, Maiello R, Tassone P, Buresti G, et al. (2015). Investigation on cobalt-oxide nanoparticles cyto-genotoxicity and inflammatory response in two types of respiratory cells. *J Appl Toxicol*. 35(10):1102–13. doi:10.1002/jat.3133 PMID:25772588

Chang YC, Lin CW, Hsieh MC, Wu HJ, Wu WS, Wu WC, et al. (2017). High mobility group B1 up-regulates angiogenic and fibrogenic factors in human retinal pigment

epithelial ARPE-19 cells. *Cell Signal*. 40:248–57. doi:10.1016/j.cellsig.2017.09.019 PMID:28970183

Chen CL, Chu JS, Su WC, Huang SC, Lee WY (2010a). Hypoxia and metabolic phenotypes during breast carcinogenesis: expression of HIF-1α, GLUT1, and CAIX. *Virchows Arch*. 457(1):53–61. doi:10.1007/s00428-010-0938-0 PMID:20526721

Chen DW, Wang H, Bao YF, Xie K (2018a). Notch signaling molecule is involved in the invasion of MiaPaCa2 cells induced by $CoCl_2$ via regulating epithelial-mesenchymal transition. *Mol Med Rep*. 17(4):4965–72. doi:10.3892/mmr.2018.8502 PMID:29393429

Chen F, Chen R, Liu H, Sun R, Huang J, Huang Z, et al. (2017a). BMP-7 ameliorates cobalt alloy particle-induced inflammation by suppressing Th17 responses. *APMIS*. 125(10):880–7. doi:10.1111/apm.12730 PMID:28736908

Chen J, Han TL, Zhou X, Baker P, Shao Y, Zhang H (2020). Metabolic disparities of different oxidative stress-inducing conditions in HTR8/SVneo cells. *Mol Med Rep*. 21(2):540–8. doi:10.3892/mmr.2019.10861 PMID:31974599

Chen LJ, Ito S, Kai H, Nagamine K, Nagai N, Nishizawa M, et al. (2017b). Microfluidic co-cultures of retinal pigment epithelial cells and vascular endothelial cells to investigate choroidal angiogenesis. *Sci Rep*. 7(1):3538. doi:10.1038/s41598-017-03788-5 PMID:28615726

Cheng Y, Chen G, Hong L, Zhou L, Hu M, Li B, et al. (2013). How does hypoxia inducible factor-1α participate in enhancing the glycolysis activity in cervical cancer? *Ann Diagn Pathol*. 17(3):305–11. doi:10.1016/j.anndiagpath.2012.12.002 PMID:23375385

Christova T, Duridanova D, Braykova A, Setchenska M, Bolton T (2001). Heme oxygenase is the main protective enzyme in rat liver upon 6-day administration of cobalt chloride. *Arch Toxicol*. 75(8):445–51. doi:10.1007/s002040100253 PMID:11757667

Christova TY, Duridanova DB, Setchenska MS (2002). Enhanced heme oxygenase activity increases the antioxidant defense capacity of guinea pig liver upon acute cobalt chloride loading: comparison with rat liver. *Comp Biochem Physiol C Toxicol Pharmacol*. 131(2):177–84. doi:10.1016/S1532-0456(01)00287-3 PMID:11879785

Christova TY, Gorneva GA, Taxirov SI, Duridanova DB, Setchenska MS (2003). Effect of cisplatin and cobalt chloride on antioxidant enzymes in the livers of Lewis lung carcinoma-bearing mice: protective role of heme oxygenase. *Toxicol Lett*. 138(3):235–42. doi:10.1016/S0378-4274(02)00416-2 PMID:12565200

Ciğerci İH, Ali MM, Kaygısız ŞY, Liman R (2016). Genotoxicity assessment of cobalt chloride in *Eisenia hortensis* earthworms coelomocytes by comet assay and micronucleus test. *Chemosphere*. 144:754–7. doi:10.1016/j.chemosphere.2015.09.053 PMID:26408983

Clyne N, Hofman-Bang C, Haga Y, Hatori N, Marklund SL, Pehrsson SK, et al. (2001). Chronic cobalt exposure affects antioxidants and ATP production in rat myocardium. *Scand J Clin Lab Invest*. 61(8):609–14. doi:10.1080/003655101753267964 PMID:11768320

Dai M, Cui P, Yu M, Han J, Li H, Xiu R (2008). Melatonin modulates the expression of VEGF and HIF-1α induced by $CoCl_2$ in cultured cancer cells. *J Pineal Res*. 44(2):121–6. doi:10.1111/j.1600-079X.2007.00498.x PMID:18289162

Daido A, Aniya Y (1994). Alteration of liver glutathione *S*-transferase and protease activities by cobalt chloride treatment of rats. *Jpn J Pharmacol*. 66(3):357–62. doi:10.1254/jjp.66.357 PMID:7532736

Demir E, Kocaoğlu S, Cetin H, Kaya B (2009). Antigenotoxic effects of *Citrus aurentium* L. fruit peel oil on mutagenicity of two alkylating agents and two metals in the *Drosophila* wing spot test. *Environ Mol Mutagen*. 50(6):483–8. doi:10.1002/em.20484 PMID:19350605

Devitt BM, Queally JM, Vioreanu M, Butler JS, Murray D, Doran PP, et al. (2010). Cobalt ions induce chemokine secretion in a variety of systemic cell lines. *Acta Orthop*. 81(6):756–64. doi:10.3109/17453674.2010.537806 PMID:21110705

Dick CA, Brown DM, Donaldson K, Stone V (2003). The role of free radicals in the toxic and inflammatory effects of four different ultrafine particle types. *Inhal Toxicol*. 15(1):39–52. doi:10.1080/08958370304454 PMID:12476359

Díez-Tercero L, Delgado LM, Bosch-Rué E, Perez RA (2021). Evaluation of the immunomodulatory effects of cobalt, copper and magnesium ions in a pro inflammatory environment. *Sci Rep*. 11(1):11707. doi:10.1038/s41598-021-91070-0 PMID:34083604

Egilsson V, Evans IH, Wilkie D (1979). Toxic and mutagenic effects of carcinogens on the mitochondria of *Saccharomyces cerevisiae*. *Mol Gen Genet*. 174(1):39–46. doi:10.1007/BF00433303 PMID:384160

Eltit F, Noble J, Sharma M, Benam N, Haegert A, Bell RH, et al. (2021). Cobalt ions induce metabolic stress in synovial fibroblasts and secretion of cytokines/chemokines that may be diagnostic markers for adverse local tissue reactions to hip implants. *Acta Biomater*. 131:581–94. doi:10.1016/j.actbio.2021.06.039 PMID:34192572

Ertuğrul H, Yalçın B, Güneş M, Kaya B (2020). Ameliorative effects of melatonin against nano and ionic cobalt induced genotoxicity in two in vivo *Drosophila* assays. *Drug Chem Toxicol*. 43(3):279–86. doi:10.1080/01480545.2019.1585444 PMID:30880493

Erturk FA, Ay H, Nardemir G, Agar G (2013). Molecular determination of genotoxic effects of cobalt and nickel on maize (*Zea mays* L.) by RAPD and protein analyses. *Toxicol Ind Health*. 29(7):662–71. doi:10.1177/0748233712442709 PMID:22499271

Faisal M, Saquib Q, Alatar AA, Al-Khedhairy AA, Ahmed M, Ansari SM, et al. (2016). Cobalt oxide nanoparticles aggravate DNA damage and cell death in eggplant via mitochondrial swelling and NO signalling pathway. *Biol Res*. 49(1):20. doi:10.1186/s40659-016-0080-9 PMID:26988690

Feng S, Zhang Z, Mo Y, Tong R, Zhong Z, Chen Z, et al. (2020). Activation of NLRP3 inflammasome in hepatocytes after exposure to cobalt nanoparticles: the role of oxidative stress. *Toxicol In Vitro*. 69:104967. doi:10.1016/j.tiv.2020.104967 PMID:32805375

Frings VG, Müller D, Storz G, Rossi A, Sennefelder H, Adam C, et al. (2019). Improved metal allergen reactivity of artificial skin models by integration of Toll-like receptor 4-positive cells. *Contact Dermatitis*. 81(4):254–61. [Erratum in: Contact Dermatitis. 2020;82(2):136.] doi:10.1111/cod.13336 PMID:31198997

Fukunaga M, Kurachi Y, Mizuguchi Y (1982). Action of some metal ions on yeast chromosomes. *Chem Pharm Bull (Tokyo)*. 30(8):3017–9. doi:10.1248/cpb.30.3017 PMID:6754115

Garoui E, Ben Amara I, Driss D, Elwej A, Chaabouni SE, Boudawara T, et al. (2013). Effects of cobalt on membrane ATPases, oxidant, and antioxidant values in the cerebrum and cerebellum of suckling rats. *Biol Trace Elem Res*. 154(3):387–95. doi:10.1007/s12011-013-9746-0 PMID:23857379

Garoui EM, Fetoui H, Ayadi Makni F, Boudawara T, Zeghal N (2011). Cobalt chloride induces hepatotoxicity in adult rats and their suckling pups. *Exp Toxicol Pathol*. 63(1–2):9–15. doi:10.1016/j.etp.2009.09.003 PMID:19819122

Gibbs S, Kosten I, Veldhuizen R, Spiekstra S, Corsini E, Roggen E, et al. (2018). Assessment of metal sensitizer potency with the reconstructed human epidermis IL-18 assay. *Toxicology*. 393:62–72. doi:10.1016/j.tox.2017.10.014 PMID:29079364

Goebeler M, Meinardus-Hager G, Roth J, Goerdt S, Sorg C (1993). Nickel chloride and cobalt chloride, two common contact sensitizers, directly induce expression of intercellular adhesion molecule-1 (ICAM-1), vascular cell adhesion molecule-1 (VCAM-1), and endothelial leukocyte adhesion molecule (ELAM-1) by endothelial cells. *J Invest Dermatol*. 100(6):759–65. doi:10.1111/1523-1747.ep12476328 PMID:7684425

Gonzales S, Polizio AH, Erario MA, Tomaro ML (2005). Glutamine is highly effective in preventing in vivo cobalt-induced oxidative stress in rat liver. *World J Gastroenterol*. 11(23):3533–8. doi:10.3748/wjg.v11.i23.3533 PMID:15962369

Gori C, Zucconi L (1957). Cytological activity induced by a group of inorganic compounds in *Allium cepa*. *Caryologia*. 10:29–45. [Italian] doi:10.1080/00087114.1957.10797611

Gray MJ, Zhang J, Ellis LM, Semenza GL, Evans DB, Watowich SS, et al. (2005). HIF-1α, STAT3, CBP/p300 and Ref-1/APE are components of a transcriptional complex that regulates Src-dependent hypoxia-induced expression of VEGF in pancreatic and prostate carcinomas. *Oncogene*. 24(19):3110–20. doi:10.1038/sj.onc.1208513 PMID:15735682

Gu Y, Liu W, Liu G, Li X, Lu P (2021). Assessing the protective effects of cryptotanshinone on $CoCl_2$-induced hypoxia in RPE cells. *Mol Med Rep*. 24(4):739. doi:10.3892/mmr.2021.12379 PMID:34435647

Guan D, Su Y, Li Y, Wu C, Meng Y, Peng X, et al. (2015). Tetramethylpyrazine inhibits $CoCl_2$ -induced neurotoxicity through enhancement of Nrf2/GCLc/GSH and suppression of HIF1α/NOX2/ROS pathways. *J Neurochem*. 134(3):551–65. doi:10.1111/jnc.13161 PMID:25952107

Guildford AL, Poletti T, Osbourne LH, Di Cerbo A, Gatti AM, Santin M (2009). Nanoparticles of a different source induce different patterns of activation in key biochemical and cellular components of the host response. *J R Soc Interface*. 6(41):1213–21. doi:10.1098/rsif.2009.0021 PMID:19324665

Han YH, Xia L, Song LP, Zheng Y, Chen WL, Zhang L, et al. (2006). Comparative proteomic analysis of hypoxia-treated and untreated human leukemic U937 cells. *Proteomics*. 6(11):3262–74. doi:10.1002/pmic.200500754 PMID:16622835

Hatori N, Pehrsson SK, Clyne N, Hansson G, Hofman-Bang C, Marklund SL, et al. (1993). Acute cobalt exposure and oxygen radical scavengers in the rat myocardium. *Biochim Biophys Acta*. 1181(3):257–60. doi:10.1016/0925-4439(93)90029-Z PMID:8391326

Inoue T, Ohta Y, Sadaie Y, Kada T (1981). Effect of cobaltous chloride on spontaneous mutation induction in a *Bacillus subtilis* mutator strain. *Mutat Res*. 91(1):41–5. doi:10.1016/0165-7992(81)90068-3 PMID:6782475

Johansson A, Lundborg M, Wiernik A, Jarstrand C, Camner P (1986). Rabbit alveolar macrophages after long-term inhalation of soluble cobalt. *Environ Res*. 41(2):488–96. doi:10.1016/S0013-9351(86)80143-8 PMID:3780647

Kada T, Kanematsu N (1978). Reduction of *N*-methyl-*N*′-nitro-*N*-nitrosoguanidine-induced mutations by cobalt chloride in *Escherichia coli*. *Proc Jpn Acad, Ser B, Phys Biol Sci*. 54 5:234–7. doi:10.2183/pjab.54.234

Kalefetoğlu Macar T, Macar O, Yalçın E, Çavuşoğlu K (2021). Protective roles of grape seed (*Vitis vinifera L.*) extract against cobalt(II) nitrate stress in *Allium cepa* L. root tip cells. *Environ Sci Pollut Res Int*. 28(1):270–9. doi:10.1007/s11356-020-10532-6 PMID:32809124

Kaliman PA, Nikitchenko IV, Sokol OA, Strel'chenko EV (2001). Regulation of heme oxygenase activity in rat liver during oxidative stress induced by cobalt chloride and mercury chloride. *Biochemistry (Mosc)*. 66(1):77–82. doi:10.1023/A:1002889814723 PMID:11240397

Kalinich JF, Vergara VB, Hoffman JF (2022). Serum indicators of oxidative damage from embedded metal fragments in a rat model. *Oxid Med Cell Longev.* 2022:5394303. doi:10.1155/2022/5394303 PMID:35154566

Kalpana S, Dhananjay S, Anju B, Lilly G, Sai Ram M (2008). Cobalt chloride attenuates hypobaric hypoxia induced vascular leakage in rat brain: molecular mechanisms of action of cobalt chloride. *Toxicol Appl Pharmacol.* 231(3):354–63. doi:10.1016/j.taap.2008.05.008 PMID:18635243

Kanematsu N, Hara M, Kada T (1980). Rec assay and mutagenicity studies on metal compounds. *Mutat Res.* 77(2):109–16. doi:10.1016/0165-1218(80)90127-5 PMID:6769036

Kappas A, Drummond GS, Sardana MK (1985). Sn-protoporphyrin rapidly and markedly enhances the heme saturation of hepatic tryptophan pyrrolase. Evidence that this synthetic metalloporphyrin increases the functional content of heme in the liver. *J Clin Invest.* 75(1):302–5. doi:10.1172/JCI111689 PMID:3965510

Karri V, Lidén C, Fyhrquist N, Högberg J, Karlsson HL (2021). Impact of mono-culture vs. co-culture of keratinocytes and monocytes on cytokine responses induced by important skin sensitizers. *J Immunotoxicol.* 18(1):74-84. doi:10.1080/1547691X.2021.1905754 PMID:34019775

Kasprzak KS, Zastawny TH, North SL, Riggs CW, Diwan BA, Rice JM, et al. (1994). Oxidative DNA base damage in renal, hepatic, and pulmonary chromatin of rats after intraperitoneal injection of cobalt(II) acetate. *Chem Res Toxicol.* 7(3):329–35. doi:10.1021/tx00039a009 PMID:8075364

Kawanishi S, Inoue S, Yamamoto K (1989b). Hydroxyl radical and singlet oxygen production and DNA damage induced by carcinogenic metal compounds and hydrogen peroxide. *Biol Trace Elem Res.* 21(1):367–72. doi:10.1007/BF02917277 PMID:2484615

Kawanishi S, Yamamoto K, Inoue S (1989a). Site-specific DNA damage induced by sulfite in the presence of cobalt(II) ion. Role of sulfate radical. *Biochem Pharmacol.* 38(20):3491–6. doi:10.1016/0006-2952(89)90119-6 PMID:2818640

Kaya B, Creus A, Velázquez A, Yanikoğlu A, Marcos R (2002). Genotoxicity is modulated by ascorbic acid. Studies using the wing spot test in *Drosophila*. *Mutat Res.* 520(1–2):93–101. doi:10.1016/S1383-5718(02)00173-0 PMID:12297148

Kewitz S, Kurch L, Volkmer I, Staege MS (2016). Stimulation of the hypoxia pathway modulates chemotherapy resistance in Hodgkin's lymphoma cells. *Tumour Biol.* 37(6):8229–37. doi:10.1007/s13277-015-4705-3 PMID:26718211

Khalil SR, El Bohi KM, Khater S, Abd El-fattah AH, Mahmoud FA, Farag MR (2020). *Moringa oleifera* leaves ethanolic extract influences DNA damage signalling pathways to protect liver tissue from cobalt -triggered apoptosis in rats. *Ecotoxicol Environ Saf.* 200:110716. doi:10.1016/j.ecoenv.2020.110716 PMID:32450433

Kharab P, Singh I (1985). Genotoxic effects of potassium dichromate, sodium arsenite, cobalt chloride and lead nitrate in diploid yeast. *Mutat Res.* 155(3):117–20. doi:10.1016/0165-1218(85)90128-4 PMID:3883155

Kharab P, Singh I (1987). Induction of respiratory deficiency in yeast by salts of chromium, arsenic, cobalt and lead. *Indian J Exp Biol.* 25(2):141–2. PMID:3311978

Kim HH, Lee SE, Chung WJ, Choi Y, Kwack K, Kim SW, et al. (2002). Stabilization of hypoxia-inducible factor-1α is involved in the hypoxic stimuli-induced expression of vascular endothelial growth factor in osteoblastic cells. *Cytokine.* 17(1):14–27. doi:10.1006/cyto.2001.0985 PMID:11886167

Kim KS, Rajagopal V, Gonsalves C, Johnson C, Kalra VK (2006b). A novel role of hypoxia-inducible factor in cobalt chloride- and hypoxia-mediated expression of IL-8 chemokine in human endothelial cells. *J Immunol.* 177(10):7211–24. doi:10.4049/jimmunol.177.10.7211 PMID:17082639

Kirkland D, Brock T, Haddouk H, Hargeaves V, Lloyd M, Mc Garry S, et al. (2015). New investigations into the genotoxicity of cobalt compounds and their impact on overall assessment of genotoxic risk. *Regul Toxicol Pharmacol.* 73(1):311–38. doi:10.1016/j.yrtph.2015.07.016 PMID:26210821

Klasson M, Lindberg M, Särndahl E, Westberg H, Bryngelsson IL, Tuerxun K, et al. (2021a). Dose- and time-dependent changes in viability and IL-6, CXCL8 and CCL2 production by HaCaT-cells exposed to cobalt. Effects of high and low calcium growth conditions. *PLoS One.* 16(6):e0252159. doi:10.1371/journal.pone.0252159 PMID:34086734

Klasson M, Lindberg M, Westberg H, Bryngelsson IL, Tuerxun K, Persson A, et al. (2021b). Dermal exposure to cobalt studied *in vitro* in keratinocytes - effects of cobalt exposure on inflammasome activated cytokines, and mRNA response. *Biomarkers.* 26(8):674–84. doi:10.1080/1354750X.2021.1975823 PMID:34496682

Knyazev E, Maltseva D, Raygorodskaya M, Shkurnikov M (2021). HIF-dependent *NFATC1* activation upregulates *ITGA5* and *PLAUR* in intestinal epithelium in inflammatory bowel disease. *Front Genet.* 12:791640. doi:10.3389/fgene.2021.791640 PMID:34858489

Kong IC, Ko KS, Koh DC, Chon CM (2020). Comparative effects of particle sizes of cobalt nanoparticles to nine biological activities. *Int J Mol Sci.* 21(18):6767. doi:10.3390/ijms21186767 PMID:32942696

Kumar V, Mishra RK, Kaur G, Dutta D (2017). Cobalt and nickel impair DNA metabolism by the oxidative stress independent pathway. *Metallomics.* 9(11):1596–609. doi:10.1039/C7MT00231A PMID:29058747

Kuno Y, Tochihara N, Koike S (1980). The effects of cobalt chloride on the formation of blood lipid peroxide related to glutathione peroxidase in the erythrocytes of rabbits. *Jpn J Hyg*. 35(4):665–9. doi:10.1265/jjh.35.665 PMID:7241837

Laumonier T, Ruffieux E, Paccaud J, Kindler V, Hannouche D (2020). In vitro evaluation of human myoblast function after exposure to cobalt and chromium ions. *J Orthop Res*. 38(6):1398–406. doi:10.1002/jor.24579 PMID:31883135

Law PC, Auyeung KK, Chan LY, Ko JK (2012). Astragalus saponins downregulate vascular endothelial growth factor under cobalt chloride-stimulated hypoxia in colon cancer cells. *BMC Complement Altern Med*. 12(1):160. doi:10.1186/1472-6882-12-160 PMID:22992293

Lawrence H, Deehan D, Holland J, Kirby J, Tyson-Capper A (2014). The immunobiology of cobalt. Demonstration of a potential aetiology for inflammatory pseudotumours after metal-on-metal replacement of the hip. *Bone Joint J*. 96-B(9):1172–7. doi:10.1302/0301-620X.96B9.33476 PMID:25183586

Lawrence H, Mawdesley AE, Holland JP, Kirby JA, Deehan DJ, Tyson-Capper AJ (2016). Targeting Toll-like receptor 4 prevents cobalt-mediated inflammation. *Oncotarget*. 7(7):7578–85. doi:10.18632/oncotarget.7105 PMID:26840091

Lee M, Hwang JT, Yun H, Kim EJ, Kim MJ, Kim SS, et al. (2006). Critical roles of AMP-activated protein kinase in the carcinogenic metal-induced expression of VEGF and HIF-1 proteins in DU145 prostate carcinoma. *Biochem Pharmacol*. 72(1):91–103. doi:10.1016/j.bcp.2006.03.021 PMID:16678800

Lee SG, Lee H, Rho HM (2001). Transcriptional repression of the human *p53* gene by cobalt chloride mimicking hypoxia. *FEBS Lett*. 507(3):259–63. doi:10.1016/S0014-5793(01)02989-1 PMID:11696352

Lewis CPL, Demedts M, Nemery B (1991). Indices of oxidative stress in hamster lung following exposure to cobalt(II) ions: in vivo and in vitro studies. *Am J Respir Cell Mol Biol*. 5(2):163–9 doi:10.1165/ajrcmb/5.2.163 PMID:1892647

Li X, Liu X, Xing Y, Zeng L, Liu X, Shen H, et al. (2022). Erianin controls collagen-mediated retinal angiogenesis via the RhoA/ROCK1 signaling pathway induced by the alpha2/beta1 integrin-collagen interaction. *Invest Ophthalmol Vis Sci*. 63(1):27. doi:10.1167/iovs.63.1.27 PMID:35060996

Li Y, Liu G, Cai D, Pan B, Lin Y, Li X, et al. (2014). H_2S inhibition of chemical hypoxia-induced proliferation of HPASMCs is mediated by the upregulation of COX-2/PGI_2. *Int J Mol Med*. 33(2):359–66. doi:10.3892/ijmm.2013.1579 PMID:24337227

Lindegren CC, Nagai S, Nagai H (1958). Induction of respiratory deficiency in yeast by manganese, copper, cobalt and nickel. *Nature*. 182(4633):446–8. doi:10.1038/182446a0 PMID:13577873

Liu HC, Chang WHS, Lin FH, Lu KH, Tsuang YH, Sun JS (1999). Cytokine and prostaglandin E_2 release from leukocytes in response to metal ions derived from different prosthetic materials: an in vitro study. *Artif Organs*. 23(12):1099–106. doi:10.1111/j.1525-1594.1999.06343.x PMID:10619928

Llesuy SF, Tomaro ML (1994). Heme oxygenase and oxidative stress. Evidence of involvement of bilirubin as physiological protector against oxidative damage. *Biochim Biophys Acta*. 1223(1):9–14. doi:10.1016/0167-4889(94)90067-1 PMID:8061058

Loboda A, Jazwa A, Wegiel B, Jozkowicz A, Dulak J (2005). Heme oxygenase-1-dependent and -independent regulation of angiogenic genes expression: effect of cobalt protoporphyrin and cobalt chloride on VEGF and IL-8 synthesis in human microvascular endothelial cells. *Cell Mol Biol (Noisy-le-grand)*. 51(4):347–55. PMID:16309584

Luo L, Petit A, Antoniou J, Zukor DJ, Huk OL, Liu RC, et al. (2005). Effect of cobalt and chromium ions on MMP-1, TIMP-1, and TNF-α gene expression in human U937 macrophages: a role for tyrosine kinases. *Biomaterials*. 26(28):5587–93. doi:10.1016/j.biomaterials.2005.02.013 PMID:15878362

Ma R, Gu Y, Groome LJ, Wang Y (2011). ADAM17 regulates TNFα production by placental trophoblasts. *Placenta*. 32(12):975–80. doi:10.1016/j.placenta.2011.09.015 PMID:22018416

Macar O, Kalefetoğlu Macar T, Çavuşoğlu K, Yalçın E (2020). Determination of protective effect of carob (*Ceratonia siliqua* L.) extract against cobalt(II) nitrate-induced toxicity. *Environ Sci Pollut Res Int*. 27(32):40253–61. doi:10.1007/s11356-020-10009-6 PMID:32661972

Maeda T, Shibai A, Yokoi N, Tarusawa Y, Kawada M, Kotani H, et al. (2021). Mutational property of newly identified mutagen L-glutamic acid γ-hydrazide in *Escherichia coli*. *Mutat Res*. 823:111759. doi:10.1016/j.mrfmmm.2021.111759 PMID:34304126

Mahkamova K, Latar N, Aspinall S, Meeson A (2018). Hypoxia increases thyroid cancer stem cell-enriched side population. *World J Surg*. 42(2):350–7. doi:10.1007/s00268-017-4331-x PMID:29167950

Maines MD, Kappas A (1974). Cobalt induction of hepatic heme oxygenase; with evidence that cytochrome *P*-450 is not essential for this enzyme activity. *Proc Natl Acad Sci USA*. 71(11):4293–7. doi:10.1073/pnas.71.11.4293 PMID:4530983

Malard V, Berenguer F, Prat O, Ruat S, Steinmetz G, Quemeneur E (2007). Global gene expression profiling in human lung cells exposed to cobalt. *BMC Genomics*. 8(1):147. doi:10.1186/1471-2164-8-147 PMID:17553155

Malard V, Chardan L, Roussi S, Darolles C, Sage N, Gaillard JC, et al. (2012). Analytical constraints for the analysis of human cell line secretomes by shotgun

proteomics. *J Proteomics*. 75(3):1043–54. doi:10.1016/j.jprot.2011.10.025 PMID:22079246

Mao ZJ, Tang QJ, Zhang CA, Qin ZF, Pang B, Wei PK, et al. (2012). Anti-proliferation and anti-invasion effects of diosgenin on gastric cancer BGC-823 cells with HIF-1α shRNAs. *Int J Mol Sci*. 13(5):6521–33. doi:10.3390/ijms13056521 PMID:22754381

Maurage CA, Adam E, Minéo JF, Sarrazin S, Debunne M, Siminski RM, et al. (2009). Endocan expression and localization in human glioblastomas. *J Neuropathol Exp Neurol*. 68(6):633–41. doi:10.1097/NEN.0b013e3181a52a7f PMID:19458546

Milosevic J, Adler I, Manaenko A, Schwarz SC, Walkinshaw G, Arend M, et al. (2009). Non-hypoxic stabilization of hypoxia-inducible factor alpha (HIF-α): relevance in neural progenitor/stem cells. *Neurotox Res*. 15(4):367–80. doi:10.1007/s12640-009-9043-z PMID:19384570

Minchenko A, Salceda S, Bauer T, Caro J (1994b). Hypoxia regulatory elements of the human vascular endothelial growth factor gene. *Cell Mol Biol Res*. 40(1):35–9. PMID:7528597

Mochizuki H, Kada T (1982). Antimutagenic action of cobaltous chloride on Trp-P-1-induced mutations in *Salmonella typhimurium* TA98 and TA1538. *Mutat Res*. 95(2–3):145–57. doi:10.1016/0027-5107(82)90253-6 PMID:6750380

Molitoris KH, Kazi AA, Koos RD (2009). Inhibition of oxygen-induced hypoxia-inducible factor-1α degradation unmasks estradiol induction of vascular endothelial growth factor expression in ECC-1 cancer cells in vitro. *Endocrinology*. 150(12):5405–14. doi:10.1210/en.2009-0884 PMID:19819950

Moorhouse CP, Halliwell B, Grootveld M, Gutteridge JMC (1985). Cobalt(II) ion as a promoter of hydroxyl radical and possible 'crypto-hydroxyl' radical formation under physiological conditions. Differential effects of hydroxyl radical scavengers. *Biochim Biophys Acta*. 843(3):261–8. doi:10.1016/0304-4165(85)90147-3 PMID:2998477

Morita H, Kuno Y, Koike S (1982). The effects of cobalt on superoxide dismutase activity, methemoglobin formation and lipid peroxide in rabbit erythrocytes. *Jpn J Hyg*. 37(3):597–600. doi:10.1265/jjh.37.597 PMID:7176165

Nackerdien Z, Kasprzak KS, Rao G, Halliwell B, Dizdaroglu M (1991). Nickel(II)- and cobalt(II)-dependent damage by hydrogen peroxide to the DNA bases in isolated human chromatin. *Cancer Res*. 51(21):5837–42. PMID:1933852

Nersisyan S, Galatenko A, Chekova M, Tonevitsky A (2021). Hypoxia-induced miR-148a downregulation contributes to poor survival in colorectal cancer. *Front Genet*. 12:662468. doi:10.3389/fgene.2021.662468 PMID:34135940

Ninomiya JT, Kuzma SA, Schnettler TJ, Krolikowski JG, Struve JA, Weihrauch D (2013). Metal ions activate vascular endothelial cells and increase lymphocyte chemotaxis and binding. *J Orthop Res*. 31(9):1484–91. doi:10.3390/nu12041031 PMID:32283757

Nishihashi K, Kawashima K, Nomura T, Urakami-Takebayashi Y, Miyazaki M, Takano M, et al. (2017). Cobalt chloride induces expression and function of breast cancer resistance protein (BCRP/ABCG2) in human renal proximal tubular epithelial cell line HK-2. *Biol Pharm Bull*. 40(1):82–7. doi:10.1248/bpb.b16-00684 PMID:28049953

Nishioka H (1975). Mutagenic activities of metal compounds in bacteria. *Mutat Res*. 31(3):185–9. doi:10.1016/0165-1161(75)90088-6 PMID:805366

Nordquist L, Friederich-Persson M, Fasching A, Liss P, Shoji K, Nangaku M, et al. (2015). Activation of hypoxia-inducible factors prevents diabetic nephropathy. *J Am Soc Nephrol*. 26(2):328–38. doi:10.1681/ASN.2013090990 PMID:25183809

Nordström G, Säljö A, Li SJ, Hasselgren PO (1990). Effects of ischemia and reperfusion on protein synthesis in livers with different glutathione levels. *Ann Surg*. 211(1):97–102. doi:10.1097/00000658-199001000-00017 PMID:2294851

NTP (2014). NTP technical report on the toxicology studies of cobalt metal (CASRN 7440-48-4) in F344/N rats and B6C3F1/N mice and toxicology and carcinogenesis studies of cobalt metal in F344/NTac rats and B6C3F1/N mice (inhalation studies), Technical Report 581. Research Triangle Park (NC), USA: National Toxicology Program. Available from: https://www.ncbi.nlm.nih.gov/books/NBK567171/, accessed 19 April 2022.

Numazawa S, Oguro T, Yoshida T, Kuroiwa Y (1989a). Synergistic induction of rat hepatic ornithine decarboxylase by multiple doses of cobalt chloride. *Chem Biol Interact*. 72(3):157–67. doi:10.1016/0009-2797(89)90002-1 PMID:2605669

Nunes SC, Lopes-Coelho F, Gouveia-Fernandes S, Ramos C, Pereira SA, Serpa J (2018). Cysteine boosters the evolutionary adaptation to $CoCl_2$ mimicked hypoxia conditions, favouring carboplatin resistance in ovarian cancer. *BMC Evol Biol*. 18(1):97. doi:10.1186/s12862-018-1214-1 PMID:29921232

Nyga A, Hart A, Tetley TD (2015). Importance of the HIF pathway in cobalt nanoparticle-induced cytotoxicity and inflammation in human macrophages. *Nanotoxicology*. 9(7):905–17. doi:10.3109/17435390.2014.991430 PMID:25676618

Ogawa HI, Ohyama Y, Ohsumi Y, Kakimoto K, Kato Y, Shirai Y, et al. (1999). Cobaltous chloride-induced mutagenesis in the *supF* tRNA gene of *Escherichia coli*. *Mutagenesis*. 14(2):249–53. doi:10.1093/mutage/14.2.249 PMID:10229930

Ogawa HI, Sakata K, Inouye T, Jyosui S, Niyitani Y, Kakimoto K, et al. (1986). Combined mutagenicity of cobalt(II) salt and heteroaromatic compounds in *Salmonella typhimurium*. *Mutat Res Genet Toxicol Test*. 172(2):97–104. doi:10.1016/0165-1218(86)90068-6 PMID:3531840

Ogawa HI, Shibahara T, Iwata H, Okada T, Tsuruta S, Kakimoto K, et al. (1994). Genotoxic activities in vivo of cobaltous chloride and other metal chlorides as assayed in the *Drosophila* wing spot test. *Mutat Res*. 320(1–2):133–40. doi:10.1016/0165-1218(94)90065-5 PMID:7506380

Oh JH, Oh J, Togloom A, Kim SW, Huh K (2013). Effects of *Ginkgo biloba* extract on cultured human retinal pigment epithelial cells under chemical hypoxia. *Curr Eye Res*. 38(10):1072–82. doi:10.3109/02713683.2013.804093 PMID:23790153

Osera C, Martindale JL, Amadio M, Kim J, Yang X, Moad CA, et al. (2015). Induction of *VEGFA* mRNA translation by $CoCl_2$ mediated by HuR. *RNA Biol*. 12(10):1121–30. doi:10.1080/15476286.2015.1085276 PMID:26325091

Oyagbemi AA, Akinrinde AS, Adebiyi OE, Jarikre TA, Omobowale TO, Ola-Davies OE, et al. (2020). Luteolin supplementation ameliorates cobalt-induced oxidative stress and inflammation by suppressing NF-κB/Kim-1 signaling in the heart and kidney of rats. *Environ Toxicol Pharmacol*. 80:103488. doi:10.1016/j.etap.2020.103488 PMID:32898663

Oyagbemi AA, Omobowale TO, Awoyomi OV, Ajibade TO, Falayi OO, Ogunpolu BS, et al. (2019). Cobalt chloride toxicity elicited hypertension and cardiac complication via induction of oxidative stress and upregulation of COX-2/Bax signaling pathway. *Hum Exp Toxicol*. 38(5):519–32. doi:10.1177/0960327118812158 PMID:30596275

Pagano DA, Zeiger E (1992). Conditions for detecting the mutagenicity of divalent metals in *Salmonella typhimurium*. *Environ Mol Mutagen*. 19(2):139–46. doi:10.1002/em.2850190208 PMID:1541255

Park H, Lee DS, Yim MJ, Choi YH, Park S, Seo SK, et al. (2015). 3,3′-Diindolylmethane inhibits VEGF expression through the HIF-1α and NF-κB pathways in human retinal pigment epithelial cells under chemical hypoxic conditions. *Int J Mol Med*. 36(1):301–8. doi:10.3892/ijmm.2015.2202 PMID:25955241

Peters K, Unger RE, Gatti AM, Sabbioni E, Tsaryk R, Kirkpatrick CJ (2007). Metallic nanoparticles exhibit paradoxical effects on oxidative stress and pro-inflammatory response in endothelial cells in vitro. *Int J Immunopathol Pharmacol*. 20(4):685–95. doi:10.1177/039463200702000404 PMID:18179741

Petrarca C, Perrone A, Verna N, Verginelli F, Ponti J, Sabbioni E, et al. (2006). Cobalt nano-particles modulate cytokine in vitro release by human mononuclear cells mimicking autoimmune disease. *Int J Immunopathol Pharmacol*. 19(4 Suppl):11–4. PMID:17291400

Prazmo W, Balbin E, Baranowska H, Ejchart A, Putrament A (1975). Manganese mutagenesis in yeast. II. Conditions of induction and characteristics of mitochondrial respiratory deficient *Saccharomyces cerevisiae* mutants induced with manganese and cobalt. *Genet Res*. 26(1):21–9. doi:10.1017/S0016672300015810 PMID:767216

Putrament A, Baranowska H, Ejchart A, Jachymczyk W (1977). Manganese mutagenesis in yeast. VI. Mn^{2+} uptake, mitDNA replication and E^R induction. Comparison with other divalent cations. *Mol Gen Genet*. 151(1):69–76. doi:10.1007/BF00446914 PMID:325369

Queally JM, Devitt BM, Butler JS, Malizia AP, Murray D, Doran PP, et al. (2009). Cobalt ions induce chemokine secretion in primary human osteoblasts. *J Orthop Res*. 27(7):855–64. doi:10.1002/jor.20837 PMID:19132727

Rachmawati D, Bontkes HJ, Verstege MI, Muris J, von Blomberg BME, Scheper RJ, et al. (2013). Transition metal sensing by Toll-like receptor-4: next to nickel, cobalt and palladium are potent human dendritic cell stimulators. *Contact Dermat*. 68(6):331–8. doi:10.1111/cod.12042 PMID:23692033

Reinardy HC, Syrett JR, Jeffree RA, Henry TB, Jha AN (2013). Cobalt-induced genotoxicity in male zebrafish (*Danio rerio*), with implications for reproduction and expression of DNA repair genes. *Aquat Toxicol*. 126:224–30. doi:10.1016/j.aquatox.2012.11.007 PMID:23246864

Rellinger EJ, Romain C, Choi S, Qiao J, Chung DH (2015). Silencing gastrin-releasing peptide receptor suppresses key regulators of aerobic glycolysis in neuroblastoma cells. *Pediatr Blood Cancer*. 62(4):581–6. doi:10.1002/pbc.25348 PMID:25630799

Richardson CL, Verna J, Schulman GE, Shipp K, Grant AD (1981). Metal mutagens and carcinogens effectively displace acridine orange from DNA as measured by fluorescence polarization. *Environ Mutagen*. 3(5):545–53. doi:10.1002/em.2860030506 PMID:6793355

Rossman TG, Molina M, Meyer LW (1984). The genetic toxicology of metal compounds: I. Induction of λ prophage in *E coli* $WP2_s(\lambda)$. *Environ Mutagen*. 6(1):59–69. doi:10.1002/em.2860060108 PMID:6229401

Safronova O, Nakahama K, Onodera M, Muneta T, Morita I (2003). Effect of hypoxia on monocyte chemotactic protein-1 (MCP-1) gene expression induced by Interleukin-1β in human synovial fibroblasts. [published correction appears in Inflamm Res. 53(4):170]. *Inflamm Res*. 52(11):480–6. doi:10.1007/s00011-003-1205-5 PMID:14652683

Sato A, Virgona N, Ando A, Ota M, Yano T (2014). A redox-silent analogue of tocotrienol inhibits cobalt(II) chloride-induced VEGF expression via Yes signaling in mesothelioma cells. *Biol Pharm Bull*. 37(5):865–70. doi:10.1248/bpb.b13-00846 PMID:24790010

Saxena S, Shukla D, Saxena S, Khan YA, Singh M, Bansal A, et al. (2010). Hypoxia preconditioning by cobalt chloride enhances endurance performance and protects skeletal muscles from exercise-induced oxidative damage in rats. *Acta Physiol (Oxf)*. 200(3):249–63. doi:10.1111/j.1748-1716.2010.02136.x PMID:20384596

Schmalz G, Schweikl H, Hiller KA (2000). Release of prostaglandin E_2, IL-6 and IL-8 from human oral epithelial culture models after exposure to compounds of dental materials. *Eur J Oral Sci*. 108(5):442–8. doi:10.1034/j.1600-0722.2000.108005442.x PMID:11037761

Sears JE, Hoppe G (2005). Triamcinolone acetonide destabilizes VEGF mRNA in Müller cells under continuous cobalt stimulation. *Invest Ophthalmol Vis Sci*. 46(11):4336–41. doi:10.1167/iovs.05-0565 PMID:16249516

Sheffer M, Simon AJ, Jacob-Hirsch J, Rechavi G, Domany E, Givol D, et al. (2011). Genome-wide analysis discloses reversal of the hypoxia-induced changes of gene expression in colon cancer cells by zinc supplementation. *Oncotarget*. 2(12):1191–202. doi:10.18632/oncotarget.395 PMID:22202117

Shrivastava K, Shukla D, Bansal A, Sairam M, Banerjee PK, Ilavazhagan G (2008). Neuroprotective effect of cobalt chloride on hypobaric hypoxia-induced oxidative stress. *Neurochem Int*. 52(3):368–75. doi:10.1016/j.neuint.2007.07.005 PMID:17706837

Singh I (1983). Induction of reverse mutation and mitotic gene conversion by some metal compounds in *Saccharomyces cerevisiae*. *Mutat Res*. 117(1–2):149–52. doi:10.1016/0165-1218(83)90162-3 PMID:6339905

Sirover MA, Loeb LA (1976). Metal activation of DNA synthesis. *Biochem Biophys Res Commun*. 70(3):812–7. doi:10.1016/0006-291X(76)90664-1 PMID:779784

Slomiany MG, Black LA, Kibbey MM, Day TA, Rosenzweig SA (2006). IGF-1 induced vascular endothelial growth factor secretion in head and neck squamous cell carcinoma. *Biochem Biophys Res Commun*. 342(3):851–8. doi:10.1016/j.bbrc.2006.02.043 PMID:16499871

Stelzer KJ, Klaassen CD (1985). Effect of cobalt on biliary excretion of bilirubin and glutathione. *J Toxicol Environ Health*. 15(6):813–22. doi:10.1080/15287398509530707 PMID:3840533

Stewart J, Siavash H, Hebert C, Norris K, Nikitakis NG, Sauk JJ (2003). Phenotypic switching of VEGF and collagen XVIII during hypoxia in head and neck squamous carcinoma cells. *Oral Oncol*. 39(8):862–9. doi:10.1016/S1368-8375(03)00110-6 PMID:13679210

Sumbayev VV (2001). Activities of apoptotic signal 1-regulating protein kinase and poly-(ADP-ribose) polymerase and internucleosomal DNA fragmentation in rat liver during oxidative stress induced by cobalt chloride. *Bull Exp Biol Med*. 131(2):119–20. doi:10.1023/A:1017571323899 PMID:11391389

Sun Z, Mohamed MAA, Park SY, Yi TH (2015). Fucosterol protects cobalt chloride induced inflammation by the inhibition of hypoxia-inducible factor through PI3K/Akt pathway. *Int Immunopharmacol*. 29(2):642–7. doi:10.1016/j.intimp.2015.09.016 PMID:26395918

Ton TVT, Kovi RC, Peddada TN, Chhabria RM, Shockley KR, Flagler ND, et al. (2021). Cobalt-induced oxidative stress contributes to alveolar/bronchiolar carcinogenesis in B6C3F1/N mice. *Arch Toxicol*. 95(10):3171–90. doi:10.1007/s00204-021-03146-5 PMID:34468815

Tso WW, Fung WP (1981). Mutagenicity of metallic cations. *Toxicol Lett*. 8(4-5):195–200. doi:10.1016/0378-4274(81)90100-4 PMID:7022752

Vales G, Demir E, Kaya B, Creus A, Marcos R (2013). Genotoxicity of cobalt nanoparticles and ions in *Drosophila*. *Nanotoxicology*. 7(4):462–8. doi:10.3109/17435390.2012.689882 PMID:22548285

Vengellur A, Phillips JM, Hogenesch JB, LaPres JJ (2005). Gene expression profiling of hypoxia signaling in human hepatocellular carcinoma cells. *Physiol Genomics*. 22(3):308–18. doi:10.1152/physiolgenomics.00045.2004 PMID:15942021

Verstraelen S, Remy S, Casals E, De Boever P, Witters H, Gatti A, et al. (2014). Gene expression profiles reveal distinct immunological responses of cobalt and cerium dioxide nanoparticles in two in vitro lung epithelial cell models. *Toxicol Lett*. 228(3):157–69. doi:10.1016/j.toxlet.2014.05.006 PMID:24821434

Von Rosen G (1964). Mutations induced by the action of metal ions in pisum II. Further investigations on the mutagenic action of metal ions and comparison with the activity of ionizing radiation. *Hereditas*. 51(1):89–134. doi:10.1111/j.1601-5223.1964.tb01923.x

Wan R, Mo Y, Zhang Z, Jiang M, Tang S, Zhang Q (2017). Cobalt nanoparticles induce lung injury, DNA damage and mutations in mice. *Part Fibre Toxicol*. 14(1):38. doi:10.1186/s12989-017-0219-z PMID:28923112

Wang D, Wang L, Gu J, Yang H, Liu N, Lin Y, et al. (2014). Scutellarin inhibits high glucose-induced and hypoxia-mimetic agent-induced angiogenic effects in human retinal endothelial cells through reactive oxygen species/hypoxia-inducible factor-1α/vascular endothelial growth factor pathway. *J Cardiovasc Pharmacol*. 64(3):218–27. doi:10.1097/FJC.0000000000000109 PMID:25192544

Wang JY, Wicklund BH, Gustilo RB, Tsukayama DT (1996b). Titanium, chromium and cobalt ions modulate the release of bone-associated cytokines by human monocytes/macrophages in vitro. *Biomaterials*. 17(23):2233–40. doi:10.1016/0142-9612(96)00072-5 PMID:8968517

Wang K, Lei J, Zou J, Xiao H, Chen A, Liu X, et al. (2013a). Mipu1, a novel direct target gene, is involved in hypoxia inducible factor 1-mediated cytoprotection. *PLoS One*. 8(12):e82827. doi:10.1371/journal.pone.0082827 PMID:24349374

Wang X, Yokoi I, Liu J, Mori A (1993). Cobalt(II) and nickel(II) ions as promoters of free radicals in vivo: detected directly using electron spin resonance spectrometry in circulating blood in rats. *Arch Biochem Biophys*. 306(2):402–6. doi:10.1006/abbi.1993.1529 PMID:8215442

Wang Y, Sang A, Zhu M, Zhang G, Guan H, Ji M, et al. (2016b). Tissue factor induces VEGF expression via activation of the Wnt/β-catenin signaling pathway in ARPE-19 cells. *Mol Vis*. 22:886–97. PMID:27499609

Wellinghausen N, Driessen C, Rink L (1996). Stimulation of human peripheral blood mononuclear cells by zinc and related cations. *Cytokine*. 8(10):767–71. doi:10.1006/cyto.1996.0102 PMID:8980878

Wen Z, Huang C, Xu Y, Xiao Y, Tang L, Dai J, et al. (2016). α-Solanine inhibits vascular endothelial growth factor expression by down-regulating the ERK1/2-HIF-1α and STAT3 signaling pathways. *Eur J Pharmacol*. 771:93–8. doi:10.1016/j.ejphar.2015.12.020 PMID:26688571

Wong PK (1988). Mutagenicity of heavy metals. *Bull Environ Contam Toxicol*. 40(4):597–603. doi:10.1007/BF01688386 PMID:3285919

Xia M, Huang R, Sun Y, Semenza GL, Aldred SF, Witt KL, et al. (2009). Identification of chemical compounds that induce HIF-1α activity. *Toxicol Sci*. 112(1):153–63. doi:10.1093/toxsci/kfp123 PMID:19502547

Xu M, Zheng YL, Xie XY, Liang JY, Pan FS, Zheng SG, et al. (2014). Sorafenib blocks the HIF-1α/VEGFA pathway, inhibits tumor invasion, and induces apoptosis in hepatoma cells. *DNA Cell Biol*. 33(5):275–81. doi:10.1089/dna.2013.2184 PMID:24611881

Yamamoto A, Kohyama Y, Hanawa T (2002). Mutagenicity evaluation of forty-one metal salts by the *umu* test. *J Biomed Mater Res*. 59(1):176–83. doi:10.1002/jbm.1231 PMID:11745551

Yamamoto K, Inoue S, Yamazaki A, Yoshinaga T, Kawanishi S (1989). Site-specific DNA damage induced by cobalt(II) ion and hydrogen peroxide: role of singlet oxygen. *Chem Res Toxicol*. 2(4):234–9. doi:10.1021/tx00010a004 PMID:2562423

Yang C, Ling H, Zhang M, Yang Z, Wang X, Zeng F, et al. (2011a). Oxidative stress mediates chemical hypoxia-induced injury and inflammation by activating NF-κb-COX-2 pathway in HaCaT cells. *Mol Cells*. 31(6):531–8. doi:10.1007/s10059-011-1025-3 PMID:21533553

Yang C, Yang Z, Zhang M, Dong Q, Wang X, Lan A, et al. (2011b). Hydrogen sulfide protects against chemical hypoxia-induced cytotoxicity and inflammation in HaCaT cells through inhibition of ROS/NF-κB/COX-2 pathway. *PLoS One*. 6(7):e21971. doi:10.1371/journal.pone.0021971 PMID:21779360

Yang G, Xu S, Peng L, Li H, Zhao Y, Hu Y (2016). The hypoxia-mimetic agent $CoCl_2$ induces chemotherapy resistance in LOVO colorectal cancer cells. *Mol Med Rep*. 13(3):2583–9. doi:10.3892/mmr.2016.4836 PMID:26846577

Yeşilada E (2001). Genotoxicity testing of some metals in the *Drosophila* wing somatic mutation and recombination test. *Bull Environ Contam Toxicol*. 66(4):464–9. doi:10.1007/s001280029 PMID:11443308

Yıldız M, Ciğerci IH, Konuk M, Fidan AF, Terzi H (2009). Determination of genotoxic effects of copper sulphate and cobalt chloride in *Allium cepa* root cells by chromosome aberration and comet assays. *Chemosphere*. 75(7):934–8. doi:10.1016/j.chemosphere.2009.01.023 PMID:19201446

Zeiger E, Anderson B, Haworth S, Lawlor T, Mortelmans K (1992). Salmonella mutagenicity tests: V. Results from the testing of 311 chemicals. *Environ Mol Mutagen*. 19(Suppl 21):2–141. doi:10.1002/em.2850190603 PMID:1541260

Zhang H, Ji Z, Xia T, Meng H, Low-Kam C, Liu R, et al. (2012). Use of metal oxide nanoparticle band gap to develop a predictive paradigm for oxidative stress and acute pulmonary inflammation. *ACS Nano*. 6(5):4349–68. doi:10.1021/nn3010087 PMID:22502734

Zhang N, Hong B, Zhou C, Du X, Chen S, Deng X, et al. (2017). Cobalt chloride-induced hypoxia induces epithelial-mesenchymal transition in renal carcinoma cell lines. *Ann Clin Lab Sci*. 47(1):40–6. PMID:28249915

Zhang Q, Kusaka Y, Sato K, Nakakuki K, Kohyama N, Donaldson K (1998). Differences in the extent of inflammation caused by intratracheal exposure to three ultrafine metals: role of free radicals. *J Toxicol Environ Health A*. 53(6):423–38. doi:10.1080/009841098159169 PMID:9537280

Zhao C, Moreno-Nieves U, Di Battista JA, Fernandes MJ, Touaibia M, Bourgoin SG (2015a). Chemical hypoxia brings to light altered autocrine sphingosine-1-phosphate signalling in rheumatoid arthritis synovial fibroblasts. *Mediators Inflamm*. 2015:436525. doi:10.1155/2015/436525 PMID:26556954

Zhao J, Geng YU, Hua H, Cun B, Chen Q, Xi X, et al. (2015b). Fenofibrate inhibits the expression of VEGFC and VEGFR-3 in retinal pigmental epithelial cells exposed to hypoxia. *Exp Ther Med*. 10(4):1404–12. doi:10.3892/etm.2015.2697 PMID:26622498

Zheng F, Jang WC, Fung FK, Lo ACY, Wong IYH (2016). Up-regulation of ENO1 by HIF-1α in retinal pigment epithelial cells after hypoxic challenge is not involved in the regulation of VEGF secretion. *PLoS One*. 11(2):e0147961. doi:10.1371/journal.pone.0147961 PMID:26882120

Zheng F, Luo Z, Zheng C, Li J, Zeng J, Yang H, et al. (2019). Comparison of the neurotoxicity associated with cobalt nanoparticles and cobalt chloride in Wistar rats. *Toxicol Appl Pharmacol*. 369:90–9. doi:10.1016/j.taap.2019.03.003 PMID:30849457